



Recession and Morphological Changes of the Debris-Covered Milam Glacier in Gori Ganga Valley, Central Himalaya, India, Derived From Satellite Data

Suraj Mal^{1,2*}, Manish Mehta³, R. B. Singh⁴, Udo Schickhoff¹ and M. P. S. Bisht⁵

¹ CEN Center for Earth System Research and Sustainability, Institute of Geography, University of Hamburg, Hamburg, Germany, ² Department of Geography, Shaheed Bhagat Singh College, University of Delhi, New Delhi, India, ³ Centre for Glaciology, Wadia Institute of Himalayan Geology, Dehradun, India, ⁴ Department of Geography, Delhi School of Economics, University of Delhi, New Delhi, India, ⁵ Department of Geology, HNB Garhwal University, Srinagar, India

OPEN ACCESS

Edited by:

Simon Allen,
University of Zurich, Switzerland

Reviewed by:

Atanu Bhattacharya,
University of Zurich, Switzerland
Owen King,
University of Zurich, Switzerland

*Correspondence:

Suraj Mal
surajdse@gmail.com

Specialty section:

This article was submitted to
Interdisciplinary Climate Studies,
a section of the journal
Frontiers in Environmental Science

Received: 31 March 2018

Accepted: 14 March 2019

Published: 26 April 2019

Citation:

Mal S, Mehta M, Singh RB,
Schickhoff U and Bisht MPS (2019)
Recession and Morphological
Changes of the Debris-Covered Milam
Glacier in Gori Ganga Valley, Central
Himalaya, India, Derived From Satellite
Data. *Front. Environ. Sci.* 7:42.
doi: 10.3389/fenvs.2019.00042

We analyzed the recession of the Milam glacier in the Gori Ganga valley, Uttarakhand Himalaya, using historical plane-table survey maps, topographical maps, Corona image (1968), Landsat 5 TM (1990), Landsat 7 ETM+ (2001), and Sentinel 2 (2017) satellite data. We estimate that the Milam glacier has receded by 1565.4 ± 20.6 m (31.9 ± 0.4 m a^{-1}) over the period 1968–2017, while lower recession rate (21.1 ± 1.7 m a^{-1}) was observed between 2001 and 2017. The Milam glacier lost 2.27 ± 0.06 km² of its area from 1968 to 2017 due to recession. Two tributary glaciers detached from the main trunk between 1990 and 2017, which indicates glacier thinning and melting. The glacier recession also resulted in deformation of moraine ridges on either sides in lower ablation zone of Milam glacier, which is caused due to the removal of basal ice support caused by glacier melting.

Keywords: Milam glacier, Gori Ganga, climate change, morphological changes, Himalaya

INTRODUCTION

The Indian Himalayan mountain system has experienced above average warming (~ 0.9 – 1.6°C) over the last century (Bhutiyan et al., 2007, 2009; Dash et al., 2007; Bhutiyan, 2016; Schickhoff et al., 2016) as compared with the global average of 0.85°C (IPCC, 2013). As a result, Himalayan glaciers have experienced widespread accelerated recession (length and area), thinning (mass loss), detachment and fragmentation over the last century (Raina, 2010; Bolch et al., 2012, 2019; Kääb et al., 2012, 2015; Bajracharya et al., 2014a,b, 2015; Kulkarni and Karyakarte, 2014; Shukla and Qadir, 2016). Glaciers of north-western Himalaya and Karakoram mountains have, however, shown anomalous behavior (Hewitt, 2007; Gardelle et al., 2012; Bhambri et al., 2013, 2017; Quincey et al., 2015). A review of studies on Himalayan glaciers suggests spatially variable and irregular glacier response patterns across the Karakorum-Himalayan mountain (Mayewski and Jeschke, 1979; Scherler et al., 2011; Bolch et al., 2012, 2019; Kääb et al., 2012, 2015; Schickhoff et al., 2016; Azam et al., 2018). This spatially variable glacier response is linked to the spatial variability of changing climatic conditions (temperature and precipitation trends) and geomorphic factors; including local physiography, slope of glacier bed, glacier geometry, extent and thickness of debris cover, slope-aspects, elevation characteristics

and glacial lake activities (Sakai et al., 2009; Raina, 2010; Bhambri et al., 2011a; Deota et al., 2011; Scherler et al., 2011; Bolch et al., 2012, 2019; Venkatesh et al., 2013; Nainwal et al., 2016; Shukla and Qadir, 2016).

Glaciers of eastern and north-western Himalaya and Karakorum mountains receive precipitation primarily from the Indian Summer Monsoon (ISM) and the mid-latitude westerlies (MLW) respectively, while central and western Himalayan glaciers are fed by both the weather systems (Ageta and Higuchi, 1984; Ageta and Fujita, 1996; Bookhagen and Burbank, 2010; Bolch et al., 2012; Scott et al., 2019). The changes in the behavior of ISM and MLW and associated precipitation have significantly changed the snow accumulation-contribution patterns to the glaciers across the mountain chain (Owen et al., 1996; Scherler et al., 2011; Mehta et al., 2012b; Palazzi et al., 2013; Dimri et al., 2015, 2016; Bhutiyani, 2016). The ISM affected glaciers (western, central and eastern Himalaya) largely shrank, while those influenced by MLW (north-western Himalaya and Karakorum) are relatively stable and some of them even show advancement (Scherler et al., 2011; Bolch et al., 2012, 2019).

Debris-cover in the ablation zones of the Himalayan glaciers significantly modifies the glacier-atmosphere interactions and hence the melting patterns of glacier ice (Bolch et al., 2008; Scherler et al., 2011; Schmidt and Nüsser, 2012; Basnett et al., 2013; Dobhal et al., 2013). The thin (thick) debris cover in the upper (lower) ablation zone leads to high (low) glacier ice melting (Mehta et al., 2012a; Schmidt and Nüsser, 2012; Dobhal et al., 2013). In general, the debris free glaciers show relatively higher recession rates when compared to those covered with debris (Scherler et al., 2011; Shukla and Qadir, 2016). In addition, considering slope of the glacier bed as an important factor of glacier recession, several studies suggest that glaciers with steep slopes have receded at lower rates when compared to those with gentle slopes (Venkatesh et al., 2013; Nainwal et al., 2016). Further, Deota et al. (2011) suggest that south-facing glaciers have receded much faster than those facing north. The activities of pro and supraglacial lakes also accelerate glacier recession. The proglacial lakes connected with the glacier margins lead to glacier calving and hence enhanced recession (Fujita et al., 2009; Sakai et al., 2009), while supraglacial lakes significantly melt the glacier ice in the ablation zone (Basnett et al., 2013; Raj et al., 2014; Shukla and Qadir, 2016).

Despite the fact that Himalayan glaciers have significant implications on physical processes (river runoff regime, erosion rate) as well as on socio-economic conditions (agriculture, irrigation, hydropower projects) in the mountains and adjacent plains (Basnett et al., 2013; Pandey and Venkataraman, 2013; Shukla and Qadir, 2016), relatively few glaciers have been subjected to ground-based monitoring due to their poor accessibility and harsh climatic conditions (Dobhal et al., 2004; Bhambri and Bolch, 2009; Raina, 2010; Mehta et al., 2011, 2012a; Azam et al., 2012, 2018; Dobhal et al., 2013). Therefore, remote sensing satellite data such as Landsat and Indian Remote Sensing have been important base of long-term (1970s onward) and large-scale glaciological studies in the Himalaya (Bolch et al., 2008; Bhambri et al., 2011a,b; Raj, 2011; Basnett et al., 2013; Bajracharya et al., 2015; Raj et al., 2017).

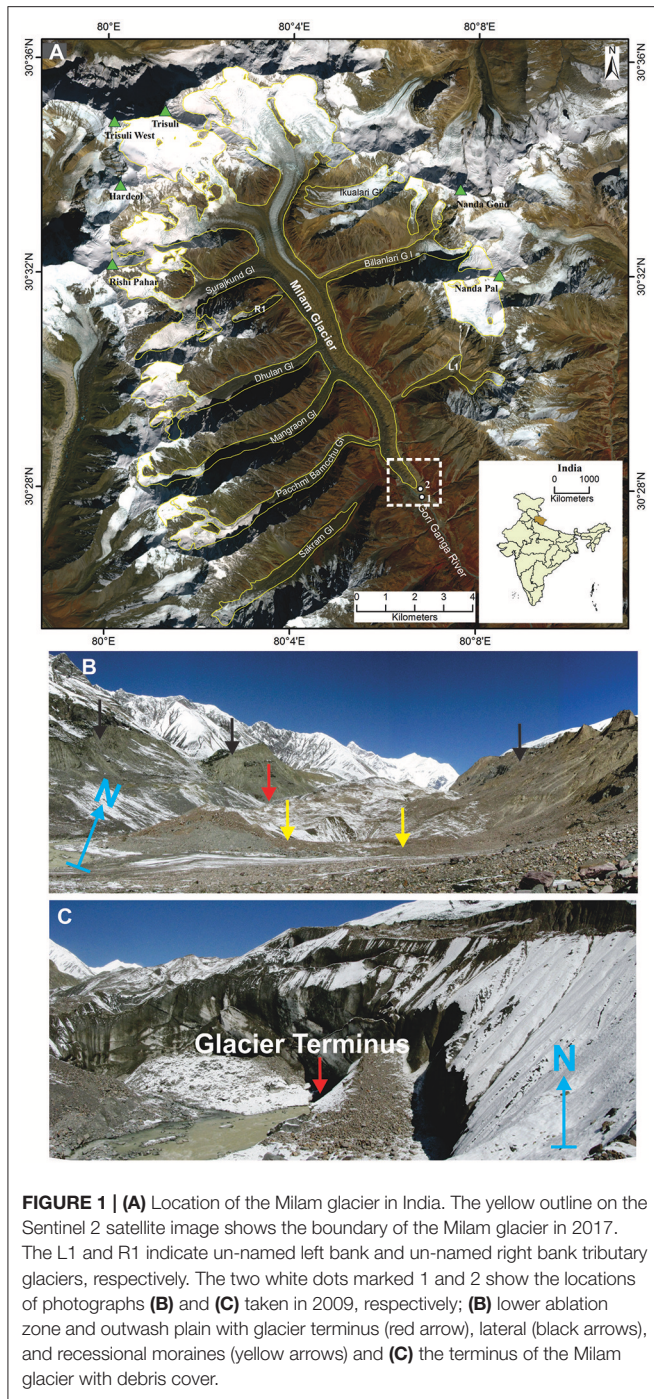
In addition, the terminus positions of some central Himalayan glaciers have been surveyed and mapped (plane-table) in the field since the early twentieth century [e.g., the Gangotri (Auden, 1937; Jangpangi, 1958); the Pindari (Cotter and Brown, 1907; Tewari and Jangpangi, 1962; Tewari, 1972); the Satopanth and Bhagirath (Jangpangi, 1958) and the Milam, Poting, Burphu, Pacchu, Shanunkalpa (Cotter and Brown, 1907; Jangpangi and Vohra, 1959; Jangpangi, 1975; Kumar et al., 1975; Shukla and Siddiqui, 2001)] (Bhambri and Bolch, 2009). These historical field-based plane-table maps of glacier terminus provide important information about their past extents, which can be compared with recent satellite images to assess the glacier recessions over a considerable time period (Bhambri and Bolch, 2009; Chand et al., 2017), for instance, Gangotri (Bhambri et al., 2012) and Satopanth and Bhagirath glaciers (Nainwal et al., 2016).

The focus of present study is on the Milam glacier, which has been subjected to field investigations and satellite data based monitoring for over a century (**Table S1**). The studies reveal that the first scientific account of glacier recession ($\sim 12.8 \text{ m a}^{-1}$, 1849–1906) was reported by Cotter and Brown (1907). Later, Mason (1939) indicated an accelerated glacier recession with $\sim 16 \text{ m a}^{-1}$ from 1906 to 1938. Significantly lower recession rates (5.6 m a^{-1}) over the period 1938–1957 were observed, which increased to $\sim 20.2 \text{ m a}^{-1}$ between 1957 and 1966 (Jangpangi and Vohra, 1959; Jangpangi, 1975; Shukla and Siddiqui, 2001). The average retreat rate over the period 1906–1966 was $\sim 13.3 \text{ m a}^{-1}$ (Jangpangi, 1975). Relatively higher recession rates (30.3 m a^{-1}) were reported from 1966 to 1997 by Shukla and Siddiqui (2001). Recent studies (Raj, 2011; Mal and Singh, 2013) reveal enhanced glacier recession rates in recent decades, while the highest recession rate (68.6 m a^{-1}) has been observed over the period 2004–2011 (Raj et al., 2014). However, we observe that there is a lack of comprehensive study, incorporating the historical maps, high resolution Corona and recent satellite data to assess the recession of the Milam glacier. We, therefore, in the present study, aim at an assessment of the recession and morphological changes of the Milam glacier in the Gori Ganga valley, Central Himalaya, India based on historical maps, high resolution Corona and recent satellite data.

MATERIALS AND METHODS

Study Area

The Milam, principal glacier in the Gori Ganga valley, is the second largest glacier ($\sim 16.2 \text{ km}$) of the Kumaon region, Uttarakhand, Central Himalaya, India (Cotter and Brown, 1907; Ahmad, 1962; Raj, 2011). Presently, the glacier covers an area of $\sim 52.7 \text{ km}^2$ between latitudes of $30^\circ 36'$ to $30^\circ 28' \text{ N}$ and longitudes of $80^\circ 00'$ to $80^\circ 07' 30'' \text{ E}$ (**Figure 1A**). The glacier originates from the south-eastern slopes of Trisuli (7,074 m), Trisuli west (7,035 m), and Hardeol (7,151 m) peaks (Ahmad, 1962; Jangpangi, 1975; Shukla and Siddiqui, 2001). It is a compound basin valley type glacier (Raj, 2011; Raj et al., 2014), which is principally fed by winter precipitation (snow) (December–February) and partly from summer precipitation (July–September), affected by MLW and ISM respectively (based



on Bookhagen and Burbank, 2010; Thayyen and Gergan, 2010; Palazzi et al., 2013). The glacier is presently fed by four tributary glaciers (Pachhmi Bamchhu ~ 7.7 km; Maogroan ~ 6 km; Dhulan ~ 6.2 km; Surajkund ~ 5.4 km) from west and one (Billanlari ~ 5.3 km) from eastern side, which are almost transverse to sub-transverse (Ahmad, 1962). The orientation of the Milam glacier is from north-west to south-east, with elevation ranging from $\sim 3,634$ m to $\sim 6,478$ m. The accumulation zone of the glacier is well developed, while the ablation zone is relatively narrow

with gentle slopes and covered under a thick layer of debris (Figure 1; Raj, 2011; Raj et al., 2014). A number of longitudinal and transverse crevasses are prominent in the accumulation and upper ablation zones (Figure 1A). Series of moraine ridges are well preserved in the region (Figure 1B), indicating temporally variable glacier extents in the past (Cotter and Brown, 1907; Ahmad, 1962; Jangpangi, 1975; Kumar et al., 1975; Shukla and Siddiqui, 2001).

Data Sources and Methods

This study is based on the historical plane-table maps of the glacier terminus, several other plane-table and topographical maps and satellite data, including high resolution Corona (1968), and moderate resolution Landsat 5 TM (1990), Landsat 7 ETM+ (2001), and Sentinel 2 (2017) images (Table 1). The historical plane-table and topographical maps were obtained from various sources, while the satellite data were obtained from the website of the United States Geological Survey (USGS) (<https://earthexplorer.usgs.gov>). The satellite scenes with low cloud and snow cover at the end of ablation season (September–November) were selected as these factors can complicate the identification of glacier outlines and lead to erroneous results (Bhambri et al., 2011a,b, 2012; Pandey and Venkataraman, 2013; Shukla and Qadir, 2016; Chand et al., 2017; Paul et al., 2017).

The gap-filled Shuttle Radar Topography Mission3 (DEM) (30 m), obtained from the website of USGS (<https://earthexplorer.usgs.gov>), was used to estimate the elevation of glacier terminus. The SRTM3 DEM has a vertical accuracy of up to 10 m (Rodriguez et al., 2006; Bhattacharya et al., 2016), while for the Indian Himalaya it is estimated to be 13.71 m between elevations of 2,000 to 4,543 m asl (Mukul et al., 2017).

The standard false color composites (FCC) of Landsat 5 TM, Landsat 7 ETM+ and Sentinel 2 satellite data were generated. Further, Landsat 7 ETM+ image was panchromatically sharpened with its 8th band using the Brovey Transform method to generate a higher spatial resolution (15 m) image (based on Bahuguna et al., 2007; Chand and Sharma, 2015). In addition, we also conducted a GPS aided field visit to the Milam glacier in October 2009 to observe various geomorphic features, such as terminus position, proglacial lakes, recessional and lateral moraines.

The station-based temperature records from the Munsyari, which is the closest station (~ 45 km air distance, 2,162 m asl) to the Milam glacier, are unavailable, while the rainfall records suffer from large data gaps (Singh and Mal, 2014). We, therefore, obtained monthly Climate Research Unit (CRU) temperature and precipitation data v4.01 (0.5×0.5 -degree, 1968–2016) for the Milam glacier region from the website of Royal Netherlands Meteorological Institute (<https://climexp.knmi.nl/>) to understand the annual and seasonal climate trends in the region. The seasonal classification scheme for Uttarakhand suggested by Basistha et al. (2009), as winters (DJF), hot summer or pre-monsoon (MAM), monsoon (JJAS) and post-monsoon (ON), has been followed in the study. The simple linear regression method was used to calculate the trends of temperature and precipitation (Kothawale and Rupa Kumar, 2005; Bhutiyani et al., 2009; Guo et al., 2016).

TABLE 1 | Details of data used in the present study.

	Type of data	Date of acquisition	Scale/spatial resolution (m)	Sources/scene ID
1	Plane-table map of the snout	1906	1':300"	Cotter and Brown, 1907
2	Plane-table map of the Milam glacier	1934	1:200,000	Shipton, 1935
3	Map of the Milam glacier	1938	1:650,000	Heim and Gansser, 1939
4	Topographical map of the Milam glacier	1954	1:250,000	US army
5	Map of the snout	1957 1966	–	Jangpangi, 1975
6	Map of the snout	1964 and Glacier outline of Mason (1939)	–	Kumar et al., 1975
7	Map of the snout	1997	1:5000	Shukla and Siddiqui, 2001
8	Corona KHA	27 Sep. 1968	4	DS1048-1134DA111_111_b DS1048-1134DF111_111_b p145r39_5t19901115
9	Landsat (5) TM	15 Nov. 1990	28.5	LE71450392001293SGS00
10	Landsat (7) ETM+ Pan	20 Oct. 2001	15	L1C_T44RMU_A012071_20171014T052639
11	Sentinel 2	14 Oct. 2017	10	

Co-registration of Maps and Satellite Data

An attempt was made to co-register all the maps and satellite images with the Sentinel 2 satellite image (14 October 2017). The plane-table map by Shipton and Tilman, published in Shipton (1935) as well as topographical maps by Heim and Gansser (1939) and the US Army (1954) were inconsistent with latest medium-high resolution satellite images due to their coarse scales, hence could not be properly co-registered (Nainwal et al., 2016). To co-register the large scale plane-table maps of the glacier terminus, the coordinate information of 1906 terminus position (Cotter and Brown, 1907) was transferred on Sentinel 2 image (14 October 2017). Based on this coordinate information and very limited commonly identifiable morphological features, an attempt was made to co-register the glacier terminus maps by Cotter and Brown (1907), Jangpangi (1975), Kumar et al. (1975), and Shukla and Siddiqui (2001). However, the co-registration results were inadequate (Nainwal et al., 2016), hence we restricted the use of field-based plane-table and topographical maps to qualitative assessments and to approximate the glacier terminus positions of 1906, 1938, 1957, and 1964. The terminus positions for other years from historical maps could not be successfully obtained. The field-based glacier terminus outlines of 1964 (Kumar et al., 1975) and 1966 (Jangpangi, 1975) were not consistent with Corona image of 1968. Nainwal et al. (2016) also mentioned similar limitations while co-registering historical topographical and field-based plane-table maps of Satopanth-Bhagirath glaciers with satellite data. Therefore, in present study, only satellite data were used for quantitative analysis of recession and morphological changes of the Milam glacier (Table 1).

Further, the subset of Corona image and other multispectral images covering the Milam glacier were co-registered with Sentinel 2 image (14 October 2017) using a total of ~36 ground control points (GCPs) taken from stable geomorphic features (Hall et al., 2003; Pandey et al., 2011; Bhambri et al., 2012; Pandey and Venkataraman, 2013; Raj et al., 2017). It has

been observed in previous studies that the corona images have significant distortions, which must be corrected before using them for glacier mapping and further analysis (Bolch et al., 2008; Bhambri et al., 2011b, 2012; Chand and Sharma, 2015; Chand et al., 2017). Thus, for precise co-registration with low error, the Corona images were co-registered with Sentinel 2 image using the two-steps approach proposed by Bhambri et al. (2011b, 2012). In the first step, the projective transformation from Sentinel 2 to Corona image based on GCPs was done, followed by the spline adjustment (Bhambri et al., 2011a; Chand et al., 2017). The co-registration errors (RMS_e) for Corona (1968), Landsat 5 TM (1990), and Landsat 7 ETM+ (2001) were 1.8 (7.2 m), 0.5 (14.25 m), and 0.5 (7.5 m), respectively.

Glacier Mapping

Several automated and semi-automated glacier mapping methods, such as band rationing, Normalized Difference Snow Index (Hall et al., 1995; Pandey et al., 2011; Bajracharya et al., 2014a,b), supervised, unsupervised (Ye et al., 2006) and object based classification (Bajracharya et al., 2014a,b, 2015; Rastner et al., 2014) have been utilized for mapping Himalayan glaciers (Bhambri and Bolch, 2009; Bhambri et al., 2011a; Pandey et al., 2011; Pandey and Venkataraman, 2013). The Morphometric Glacier Mapping (MGM) has been successfully applied for mapping large glaciers (Bolch and Kamp, 2006; Shukla et al., 2010; Bhambri et al., 2011a; Kamp et al., 2011). Several studies have even combined the MGM/band ratio with satellite thermal data to improve the accuracy of glacier mapping (Paul et al., 2004; Buchroithner and Bolch, 2007; Bhambri et al., 2011a; Alifu et al., 2015). However, obtaining a suitable threshold from such methods to map glaciers still remains a greater challenge (Alifu et al., 2015). These methods efficiently map the clean ice but often fail in debris-covered ablation zones and in the highly complex accumulation zones (e.g., ice fields) (Paul et al., 2004, 2017; Bolch and Kamp, 2006; Bhambri and Bolch, 2009; Frey

et al., 2012), leading to overestimation of glacier area (Bolch et al., 2008). Recently, coherence of SAR image combined with band ratio methods have been used for the glaciers mapping in the Himalayan region (Frey et al., 2012; Robson et al., 2015). Therefore, the glacier outlines obtained from these methods additionally require manual corrections/adjustments for the debris-covered portions and in mixed accumulation zones of glaciers (Paul et al., 2004; Bolch et al., 2008; Bhambri et al., 2011a, 2013, 2017; Alifu et al., 2015).

Therefore, manual delineation (on-screen digitization) is still a widely applied approach for glacier mapping in the heavily debris-covered ablation and mixed accumulation zones (Jin et al., 2005; Ye et al., 2006; Aizen et al., 2007; Kulkarni et al., 2007; Dutta et al., 2012; Wang et al., 2014). Nevertheless, the accuracy of manual approach (on-screen digitization) greatly depends on the skills of the operator to recognize glacier related features on the satellite images, which may result in erroneous glacier outlines (Vohra, 1980; Bhambri and Bolch, 2009; Paul et al., 2013, 2017). Therefore, Paul et al. (2013, 2017) recommend to manually map a glacier several times with a specific time interval and comparing these outlines to finalize the glacier boundaries. In present study, for maintaining the consistency of glacier outlines on different satellite images, we therefore manually digitized the glacier outlines for the years of 1968, 1990, 2001, and 2017 using different band combinations (Bhambri et al., 2011a; Pandey and Venkataraman, 2013).

Identification of Glacier Terminus

The termini of land-terminating, debris-covered Himalayan glaciers can often be difficult to distinguish from non-glaciated surrounding terrain because of their similar spectral properties (King et al., 2018). However, several surface features can be used to detect the location of a land-terminating debris covered glacier terminus e.g., (1) half-moon shaped terminus with dark colored ice wall, (2) prominent shadow from terminus, and (3) emergence of a stream from glacier (Kulkarni and Bahuguna, 2002; Bahuguna et al., 2007; Deota et al., 2011; Raj, 2011; Chand and Sharma, 2015). In case of Milam glacier, a prominent shadow from glacier terminus as well as the emergence of Gori Ganga River led to its efficient identification and mapping on various satellite images (1968, 1990, 2001, and 2017).

Glacier Length and Area Change

The changes in glacier length for various years have been measured along the glacier margins and for its terminus (Bhambri et al., 2012; Bhattacharya et al., 2016). We laid parallel lines with 50 m distance on the glacier margins in the flow direction (based on Bhambri et al., 2012; Bhattacharya et al., 2016; Mir and Majeed, 2016; Chand et al., 2017). The parallel lines between the two consecutive glacier outlines were clipped and their length were averaged for estimating the average glacier recession (Thakuri et al., 2014; Bhattacharya et al., 2016). The retreat of terminus positions for 1968–1990, 1990–2001, and 2001–2017 were calculated based on distance measured between the terminus positions of 2 years e.g., 1968–1990. The glacier outlines for different years were compared to estimate area vacated by main valley glacier as well as detachment of its

tributary glaciers. The vacated area by glacier is confined to the ablation zone. The morphological changes of moraines have been determined based on visual comparison of various satellite images.

Uncertainty Estimation

Uncertainties (errors) assessment of glacier boundaries manually digitized from satellite images with different spatial resolutions and co-registration errors is essential to substantiate the significance of the results (Bhambri et al., 2012; Pandey and Venkataraman, 2013; Shukla and Qadir, 2016). We, therefore, first calculated the absolute uncertainties for glacier length change for the image pairs based on the approach (Equation 1) of Hall et al. (2003) (e.g., Jin et al., 2005; Pandey et al., 2011; Bhambri et al., 2012, 2013; Chand et al., 2017).

$$e = \sqrt{(a)^2 + (b)^2} + E_{\text{reg}} \quad (1)$$

Where a and b are the spatial resolutions (pixel size) of image 1 and 2 respectively and E_{reg} is the error of co-registration of the satellite images. Thus, absolute uncertainties between base Sentinel 2 (2017) and Corona (1968), Landsat 5 TM (1990), Landsat 7 ETM+ (2001) were estimated as 18 m, 44.5 m, and 25.5 m, respectively. Further, the uncertainty of glacier length change from an image pair was estimated (Bhambri et al., 2012) using the Equation 2.

$$\sqrt{a^2 + b^2} \quad (2)$$

Where a and b are the absolute uncertainties of two images. The length change uncertainty between Corona (1968) and Landsat 5 TM (1990) was thus estimated as 48.0 m, between Landsat 5 TM (1990) and Landsat 7 ETM+ (2001) as 51.3 m, between Landsat 7 ETM+ (2001) and Sentinel 2 (2017) as 27.4 and between Corona (1968) and Sentinel 2 (2017) as 20.6.

The uncertainty of glacier area change was calculated using the buffer method proposed by Granshaw and Fountain (2006) (Bolch et al., 2010; Bhambri et al., 2013; Pieczonka and Bolch, 2015; Paul et al., 2017). Previous studies have suggested a buffer size of half or one pixel for uncertainty estimation of mapped glacier area from satellite data (Bolch et al., 2010; Bhambri et al., 2013; Pandey and Venkataraman, 2013; Paul et al., 2017). We selected the buffer size of 2, 14.25, 7.5, and 5 m (half pixel) for Corona (1968), Landsat TM (1990), Landsat ETM+ (2001), and Sentinel 2 (2017), respectively (following Chand and Sharma, 2015). The mapping uncertainty for the Corona (1968), Landsat TM (1990), Landsat ETM+ (2001), and Sentinel 2 were estimated as 2%, 5%, 3%, and 2%, respectively, aligning well with previous studies (Bhambri et al., 2013; Shukla and Qadir, 2016; Chand et al., 2017).

RESULTS

Glacier Retreat and Area Loss

The study reveals that the Milam glacier receded by 1565.4 ± 20.6 m from 1968 to 2017, with an average recession rate of 31.9 ± 0.4 m a^{-1} (Figure 2). The glacier recession rates over

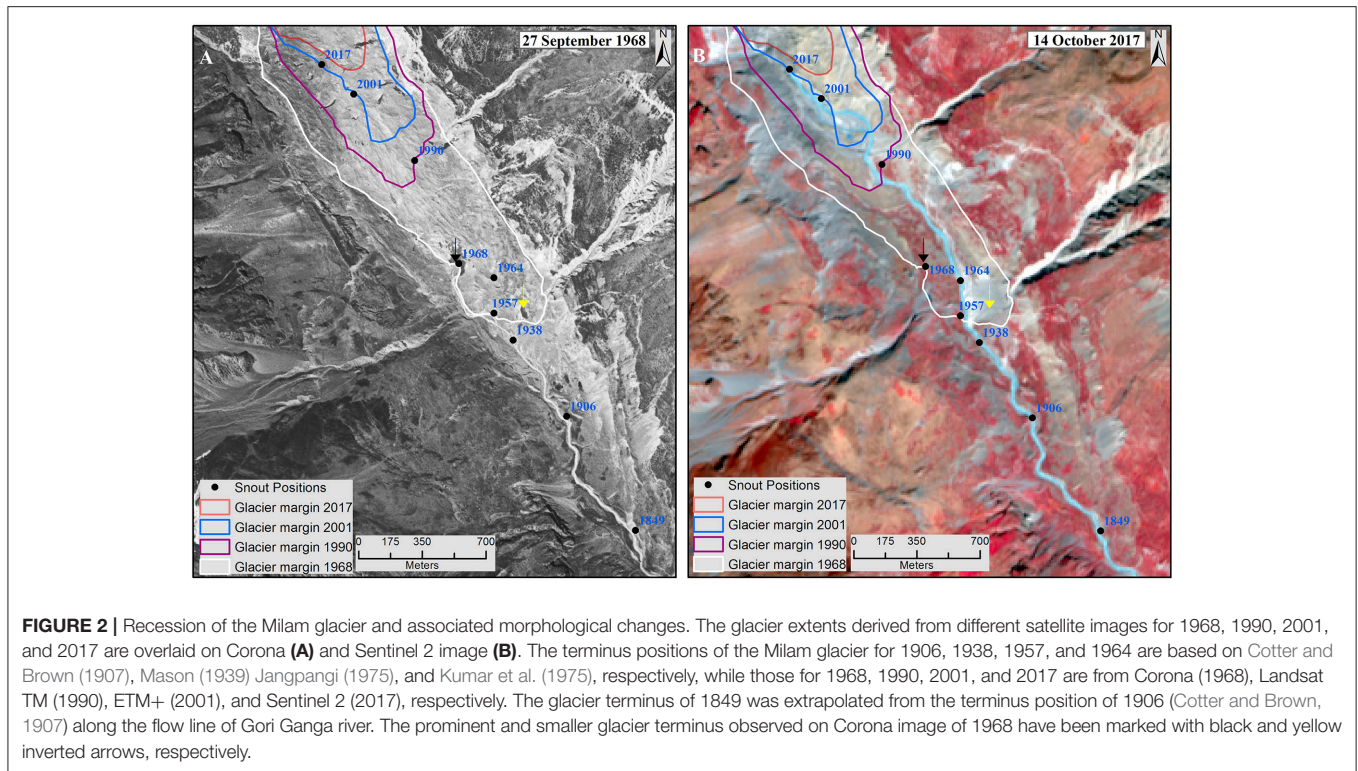


TABLE 2 | Length changes of the Milam glacier between 1968 and 2017.

Period	Total retreat (m)	Retreat rate (m a^{-1})	Retreat of active snout position (m)	Retreat rate (m a^{-1})
1968–1990	776.5 ± 48.0	35.3 ± 2.2	616.7 ± 48.0	28.0 ± 2.2
1990–2001	451.0 ± 51.3	41.0 ± 4.7	495.9 ± 51.3	45.1 ± 4.7
2001–2017	337.9 ± 27.4	21.1 ± 1.7	239.8 ± 27.4	15.0 ± 1.7
Total (1968–2017)	1565.4 ± 20.6	31.9 ± 0.4	1352.4 ± 20.6	27.6 ± 0.4

the period 1968–1990 and 1990–2001 were estimated to be $35.3 \pm 2.2 \text{ m a}^{-1}$ and $41.0 \pm 4.7 \text{ m a}^{-1}$ respectively, which were higher than the long term recession rates. The period of 1990–2001 observed highest recession rates, followed by a considerably lower rate between 2001 and 2017 ($21.1 \pm 1.7 \text{ m a}^{-1}$) (Table 2). The comparative assessments of the recession rates of the glacier margin and terminus position are presented in Table 2. The study reveals that the recession of the glacier terminus during all the study periods (except 1990–2001) was lower than that of the recession of the glacier margin. On average the glacier terminus retreated by $1352.4 \pm 20.6 \text{ m}$ ($27.6 \pm 0.4 \text{ m a}^{-1}$) over the period 1968–2017, which is $\sim 213 \text{ m}$ less than the recession of glacier margin.

The terminus position of the Milam glacier shows altitudinal shift of $\sim 178 \text{ m}$ between 1906 and 2017, which is estimated based on elevation reported by Cotter and Brown (1907) for 1906 terminus position and observed from SRTM for 2017 terminus position in the present study. About 113 m altitudinal shift of glacier terminus was observed over the period 1968–2017. In addition, the glacier terminus shows a gradual shift close to the

right lateral moraine over the study period (Figure 2). The visual interpretation of the Corona image (1968) suggests presence of two terminus positions of the Milam glacier. The prominent glacier terminus is directly related to the emergence of Gori Ganga River, whereas the smaller terminus located downstream at the lowest margin of glaciers' central flowline seems to be without any stream (Figure 2A), however for recent years only prominent terminus positions were observed over the Landsat and Sentinel 2 satellite images (Figure 2B).

The Milam glacier vacated large area in its outwash plain and along the lateral moraines in the ablation zone due to its recession and detachment of tributary glaciers. An area loss of $2.27 \pm 0.05 \text{ km}^2$ has been observed over the period 1968–2017, with an annual area loss of $0.05 \pm 0.001 \text{ km}^2$ (Table 3). A gradual increase in the area lost by the glacier has been observed from $0.03 \pm 0.002 \text{ km}^2 \text{ a}^{-1}$ over the period 1968–1990 to $0.07 \pm 0.004 \text{ km}^2 \text{ a}^{-1}$ between 1990 and 2001, which later slowed down to $0.05 \pm 0.002 \text{ km}^2 \text{ a}^{-1}$ from 2001 to 2017 (Table 3). The average annual vacated area over the period of 1990–2017 was higher than long term average (1968–2017).

TABLE 3 | Total area vacated as a result of glacier recession.

Period	Total area vacated (10^3 m^2)	Average area vacated ($10^3 \text{ m}^2 \text{ a}^{-1}$)
1968–1990	704.7 \pm 40.1	32.1 \pm 1.8
1990–2001	781.6 \pm 48.9	71.1 \pm 4.5
2001–2017	782.2 \pm 27.9	48.8 \pm 1.7
Total (1968–2017)	2268.6 \pm 48.6	46.3 \pm 0.9

Morphological Changes

Detachment of Tributary Glaciers

The study shows that the recession of the Milam glacier has resulted in the detachment of two tributary glaciers (**Figure 3**). The first right bank tributary glacier (R1, south of Surajkund glacier) detached from the Milam glacier (**Figure 3A**) after 2001. The detachment of this tributary glacier has progressed ~ 121 m by 2017 and developed its own terminus, which is presently located at $\sim 4,340$ m asl. A left bank tributary glacier (L1, opposite to Pacchmi Bamcchu glacier) detached from the Milam glacier between 1990 and 2001, and shows a surface retreat of 412 ± 27.4 m over the period 2001–2017 (**Figure 3B**). This tributary glacier has developed a terminus located at $\sim 4,038$ m asl and presently a stream emerging from it is visible on Sentinel 2 image (**Figure 3B**). In addition, the width of tributary glaciers at the confluence with the main valley glacier has been observed to decrease. For instance, the width of the confluence of Pachhmi Bamchhu tributary glacier (on the right bank) and the Milam glacier reduced by ~ 110 m between 1968 and 2017 (**Figure S1**), indicating ongoing detachment process of tributary glaciers in the region.

Changes in Moraine Ridges

We observed deformation of moraine ridges in the ablation zone of the main valley glacier between 1968 and 2017 (**Figure 4**). The right lateral moraine between the Pacchmi Bamcchu glacier and the stream from the Sakram glacier has deformed to the greater extent. Similarly, the left lateral moraine close to the present glacier terminus position shows significant deformations. Further, we observed increased exposure of moraine ridges on either sides of the Milam glacier in the lower ablation zone over the period 1968–2017 (**Figures 3, 4**). Previous studies on the Milam glacier also made similar observations about the modification and increased exposure of lateral moraines caused by glacier recession (Cotter and Brown, 1907; Ahmad, 1962; Jangpangi, 1975; Kumar et al., 1975; Raj, 2011).

DISCUSSION

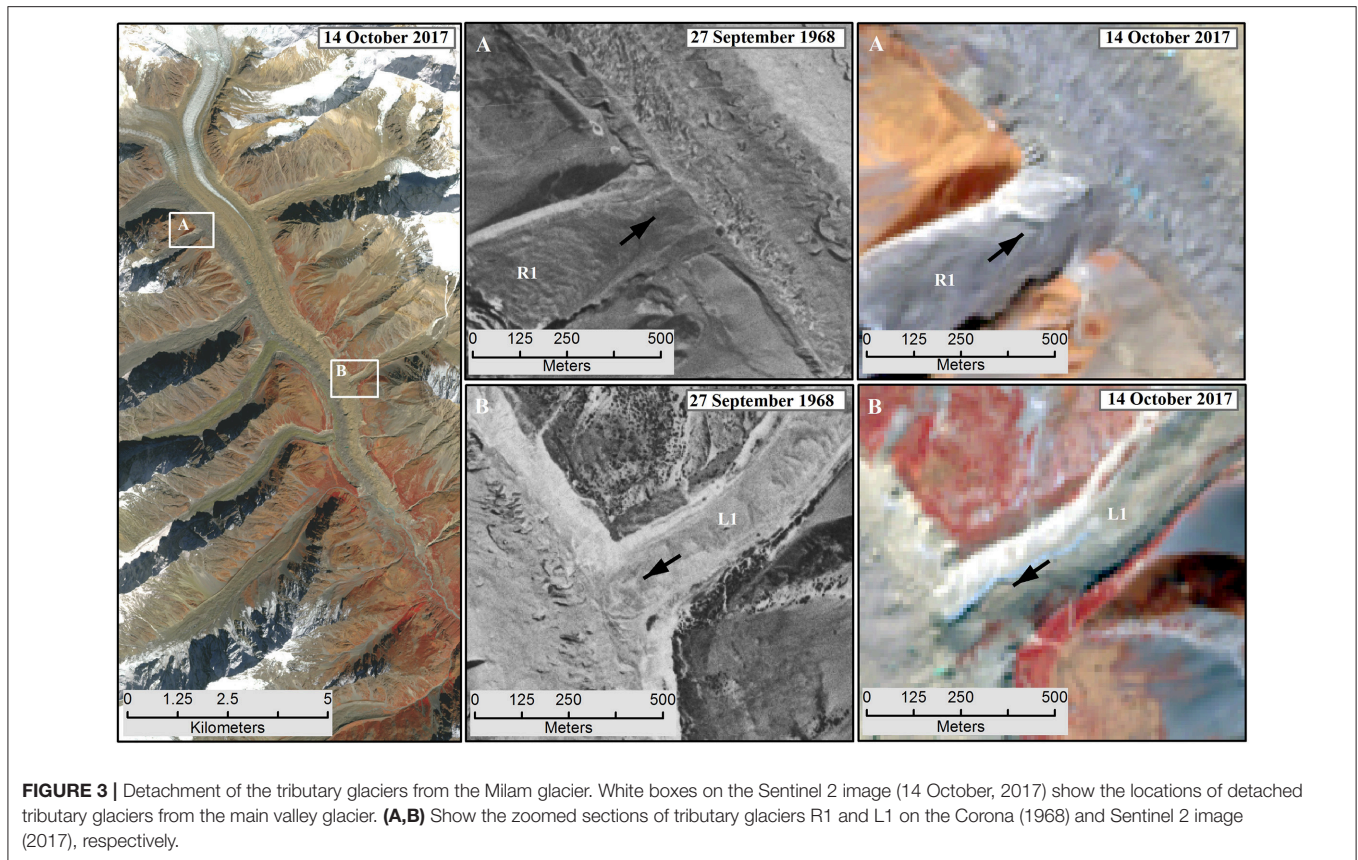
Glacier Changes and Comparison With Other Himalayan Glaciers

A review of previous studies on the Milam glacier reveals an overall receding trend, however recession rate enhanced in recent decades (**Table S1**). Our results indicating glacier recession for the period of 1968–2017 are overall consistent with previous studies on the Milam glacier (**Figure 5A**) and other nearby

Himalayan glaciers (**Figure 5B**). However, the observed glacier recession rate ($31.9 \pm 0.4 \text{ m a}^{-1}$ for 1968–2017) in this study is relatively higher than those observed by previous studies on the Milam glacier and for other nearby Himalayan glaciers (**Figure 5B**). According to Raj (2011) and Mal and Singh (2013), the Milam glacier receded by 25.5 m and 29.4 m a^{-1} over the period 1954–2006 and 1954–2009, respectively. The difference in the observed recession rates in this study and previous studies on the Milam glacier might be the result of the fact that previous studies compared the glacier extents on the coarse scale (1:250,000) topographic map (1954) with recent coarse-moderate resolution satellite images (57–15 m pixel) (**Table S1**), while this study is based on the high-moderate resolution (4–30 m pixel size) satellite data (**Table 1**). The topographical maps for pre-1970s, in many cases, have been proved to have erroneous glacier length and area records (Vohra, 1980; Bhambri and Bolch, 2009; Chand and Sharma, 2015), therefore their comparison with recent satellite images can yield suboptimal results (Bhambri et al., 2012; Nainwal et al., 2016). The high resolution Corona images have been used as an alternate to SOI maps to overcome accuracy issues (Mir and Majeed, 2016; Chand et al., 2017).

The overall higher recession rates observed for the Milam glacier in this study (1968 to 2017) might be linked to enhanced melting by seasonally active streams terminating in the lower ablation zone and outwash plain, which was previously covered by the glacier (Mehta et al., 2011; Dumka et al., 2013; Mal and Singh, 2013). Another important factor of higher glacier recession rate can be related with presence and growth of number of supraglacial lakes (~ 47) in the lower ablation zone and ongoing changes in the proglacial lakes in the region (Raj et al., 2014). A study by Nie et al. (2017) shows higher growth rate (23%) of glacial lakes in the central Himalaya compared with other Himalayan regions. The supraglacial lakes enhance the glacier melting and lower the glacier surface in the ablation zone (Bolch et al., 2008; Basnett et al., 2013; Raj et al., 2014; Shukla and Qadir, 2016), while the proglacial lakes connected with glaciers accelerate the recession of glacier terminus, e.g., Imja and Lumding (Bajracharya et al., 2007; Bajracharya and Mool, 2009; Fujita et al., 2009; Sakai et al., 2009; King et al., 2017, 2018). Prevailing winds in the valleys generate waves in these lakes, thereby increasing their activity and hence influence on the glacier recession (Fujita et al., 2009). Other glaciers in the nearby regions such as Dokriani, Tipra, Chorabari, Pindari, Gangotri, Chaturangi, Raktvarn, Satopanth, Bhagirath, Bara, and Chhota Shigri (**Figure 5B** and references cited therein) receded at comparatively lower rates over last five decades due to limited or absence of similar factors.

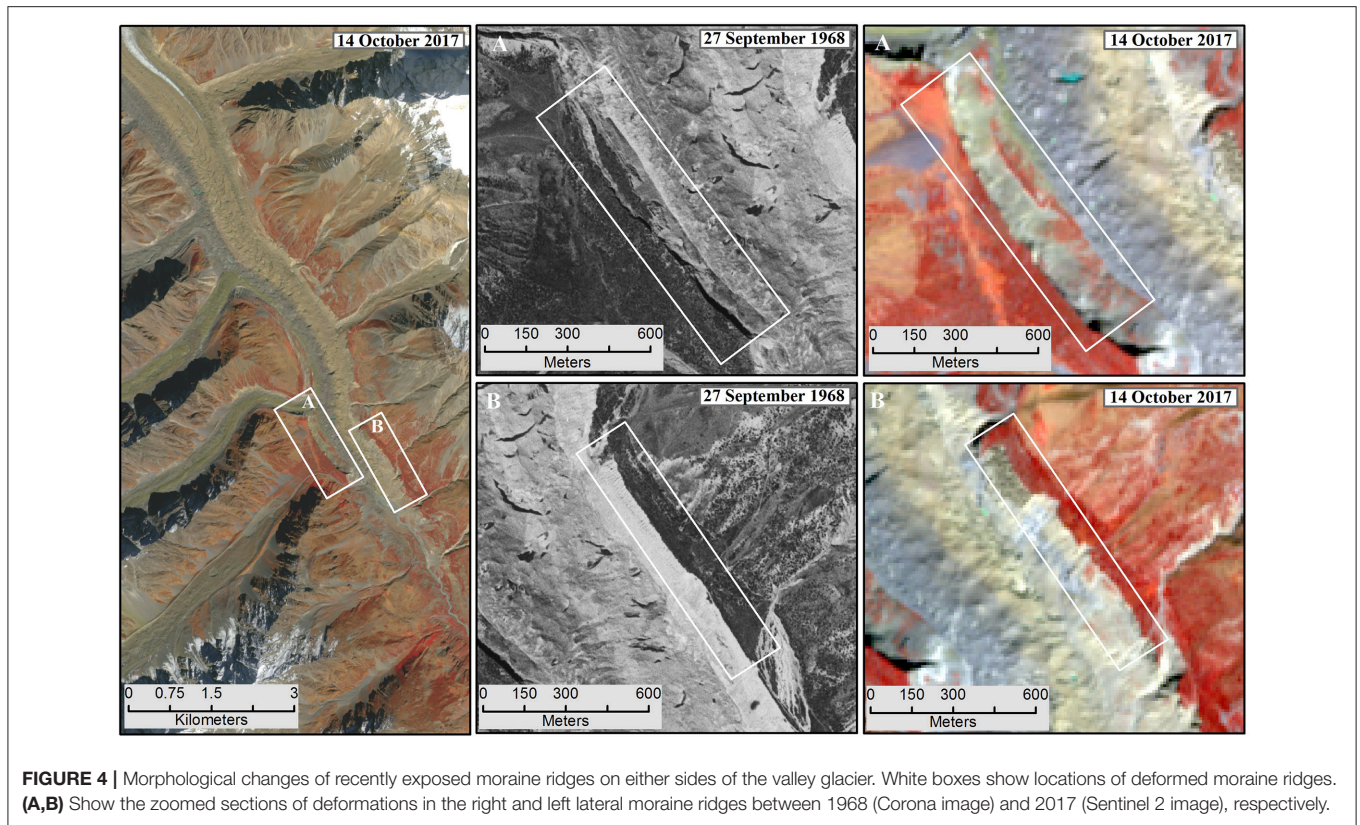
Nevertheless, our study suggests slowing down of the recession rate ($21.1 \pm 1.7 \text{ m a}^{-1}$) of the Milam glacier recently (2001–2017), while previous studies (Raj, 2011; Raj et al., 2014) showed considerably higher recession rates ($>42 \text{ m a}^{-1}$) over the period 1999–2011. This difference in observed glacier recession rates in recent decades may be attributed to (1) the interpretations of the glacier terminus outline over satellite images, (2) difference in the adopted methods, (3) satellite data with different spatial resolutions, and (4) different time periods considered in these studies (Vohra, 1980; Bhambri and



Bolch, 2009; Paul et al., 2013, 2017). We estimated glacier recession along the glacier margin based on the average method between 2001 and 2017 (Bhambri et al., 2012; Chand and Sharma, 2015; Bhattacharya et al., 2016; Chand et al., 2017), while previous studies calculated the recession of terminus position over the period 1999–2006 and 2004–2011 (Raj, 2011; Raj et al., 2014). Comparison of satellite data with different spatial resolutions (pixel size) can yield significant differences in estimated glacier recession rates (Hall et al., 2003; Shukla and Qadir, 2016), therefore these studies are not directly comparable. However, the glacier recession observed based on average method are more robust (Bhambri et al., 2012; Thakuri et al., 2014; Bhattacharya et al., 2016). In line with our findings, lower glacier recession rates in recent decades have been also reported for many large glaciers (>15 km length) which were analyzed based on similar satellite data and methods, e.g., Gangotri, Raktvarn, Chaturangi; Satopanth, Bhagirath, and Bara Shigri glaciers (Bhambri et al., 2012; Bhattacharya et al., 2016; Nainwal et al., 2016; Chand et al., 2017). However, in order to better understand the lower recession of the Milam glacier in recent decades, a regional scale geodetic mass balance study is required to evaluate the mass loss rates of glaciers across the catchment and therefore allow a comparison of glacier retreat considering various glacier attributes (Azam et al., 2012, 2018; Bhambri et al., 2012; Dobhal et al., 2013; Mehta et al., 2014; Bhattacharya et al., 2016).

The satellite image based present study reveals that the Milam glacier lost an area of $2.27 \pm 0.06 \text{ km}^2$ from 1968 to 2017, which is significantly lower ($\sim 0.61 \text{ km}^2$) than the previous estimates (Mal and Singh, 2013) that were based on comparison of coarse scale (1:250,000) topographical map of 1954 and medium resolution Aster satellite data. Our estimates, however, are significantly higher for 1968–2001 ($\sim 1.5 \text{ km}^2$), than those estimated by Shukla and Siddiqui (2001) for 1966–1997 ($\sim 0.59 \text{ km}^2$), which can be explained from the fact that we considered area vacated by terminus position, detachment of tributary glaciers as well as along the lateral moraines in the ablation zone, whereas Shukla and Siddiqui (2001) focused on the area vacated by terminus recession.

A comparison of long-term area loss results for Milam glacier and for other large glaciers (>50 km²) e.g., Gangotri and Bara Shigri reveal comparatively higher area loss than by smaller glaciers (<15 km²) (Figure 6 and references cited therein). For instance, the overall area of the Gangotri glacier shrank by $4.4 \pm 2.7 \text{ km}^2$ over the period 1968–2006 (Bhambri et al., 2011a), while its frontal area loss was estimated to be ~ 0.41 to ~ 0.47 (Bhambri et al., 2012; Bhattacharya et al., 2016). Similarly, the Bara Shigri glacier lost $1.1 \pm 0.01 \text{ km}^2$ area over the period 1965–2014, while the area lost over the period 1863–2014 is estimated to be $4 \pm 0.6 \text{ km}^2$ (Chand et al., 2017). Another study by Raj et al. (2017) suggests that the area loss of the Khatling glacier between 1965 and 2014 is $4.39 \pm 0.1 \text{ km}^2$. It is, therefore, inferred that the area



lost by the glaciers depend on their surface area (Figure 6; Basnett et al., 2013; Shukla and Qadir, 2016).

Glacier Detachment and Comparison With Other Regions

We observed detachment of two tributary glaciers from the main valley glacier. Previous studies on the Milam glacier have also reported the detachment process of tributary glaciers from the trunk of main glacier (Jangpangi, 1975; Kumar et al., 1975). The Ikualari, a left bank tributary glacier in the valley head, detached between 1957 and 1966 (Jangpangi, 1975). Kumar et al. (1975) reported that the Sakram, a right bank tributary glacier, had detached from the main valley glacier before 1964. The Sakram glacier is shown detached in the US army map of 1954 (1:250,000), while it was observed to join the valley glacier on the maps of 1934 (1:200,000) (Shipton, 1935) and 1938 (1:650,000) by Heim and Gansser (1939). Therefore, it is inferred that the Sakram glacier must have detached between 1938 and 1954. Further, Cotter and Brown (1907) indicated that 9 tributary glaciers joined the Milam glacier, while there are presently only five tributaries, suggesting the detachment of tributary glaciers over the last century. In addition, the decreasing width at the confluence of tributary glaciers and main valley glacier (e.g., Pachhmi Bamchhu) also suggest ongoing thinning and detachment (Figure S1). The detachment of tributary glaciers and ongoing thinning at their confluence with the main valley glacier have been resulted from two processes, (1) significant

melting and surface lowering of main valley glacier and (2) reduction in glacier mass turnover due to decline in the ice supply from accumulation zones to ablation zone, caused through rising temperature and precipitation changes (Salerno et al., 2015; Bolch et al., 2019). The increased exposure of lateral moraine ridges as reported by previous studies (Ahmad, 1962; Jangpangi, 1975; Kumar et al., 1975; Raj, 2011) and also through satellite image interpretation in this study support our understanding of these physical processes during last century in the study regions (Figures 3, 4). Studies have already confirmed negative mass balance of valley glaciers in nearby Himalayan region (Azam et al., 2018; Bolch et al., 2019) and significant thinning e.g., Gangotri (10.5 ± 7.2 m) between 1968 and 2014 (Bhattacharya et al., 2016) and glaciers in the Everest region (-13.3 ± 2.5 m) between 1970 and 2007 (Bolch et al., 2011). Significant ongoing glacier thinning (0.38 ± 0.06 m a^{-1}) between 2003 and 2009 in the region has been recently reported (Kääb et al., 2015), while Brun et al. (2017) revealed negative mass balance (-0.34 ± 0.09 m w.e. a^{-1}) between 2000 and 2016.

Other studies in the region have also reported detachment of tributary glaciers from the valley glacier, e.g., Tipra-Rataban (Mehta et al., 2011), Gangotri (Bhattacharya et al., 2016). As a result of detachment process, the number of glaciers in the Bhilangna basin increased from 20 to 30 over the period 1965–2014 (Raj et al., 2017), while in the Alaknanda basin from 69 to 75 over the period 1968–2006 (Bhambri et al., 2011b). Another study by Bajracharya et al. (2014b) indicated that the number of

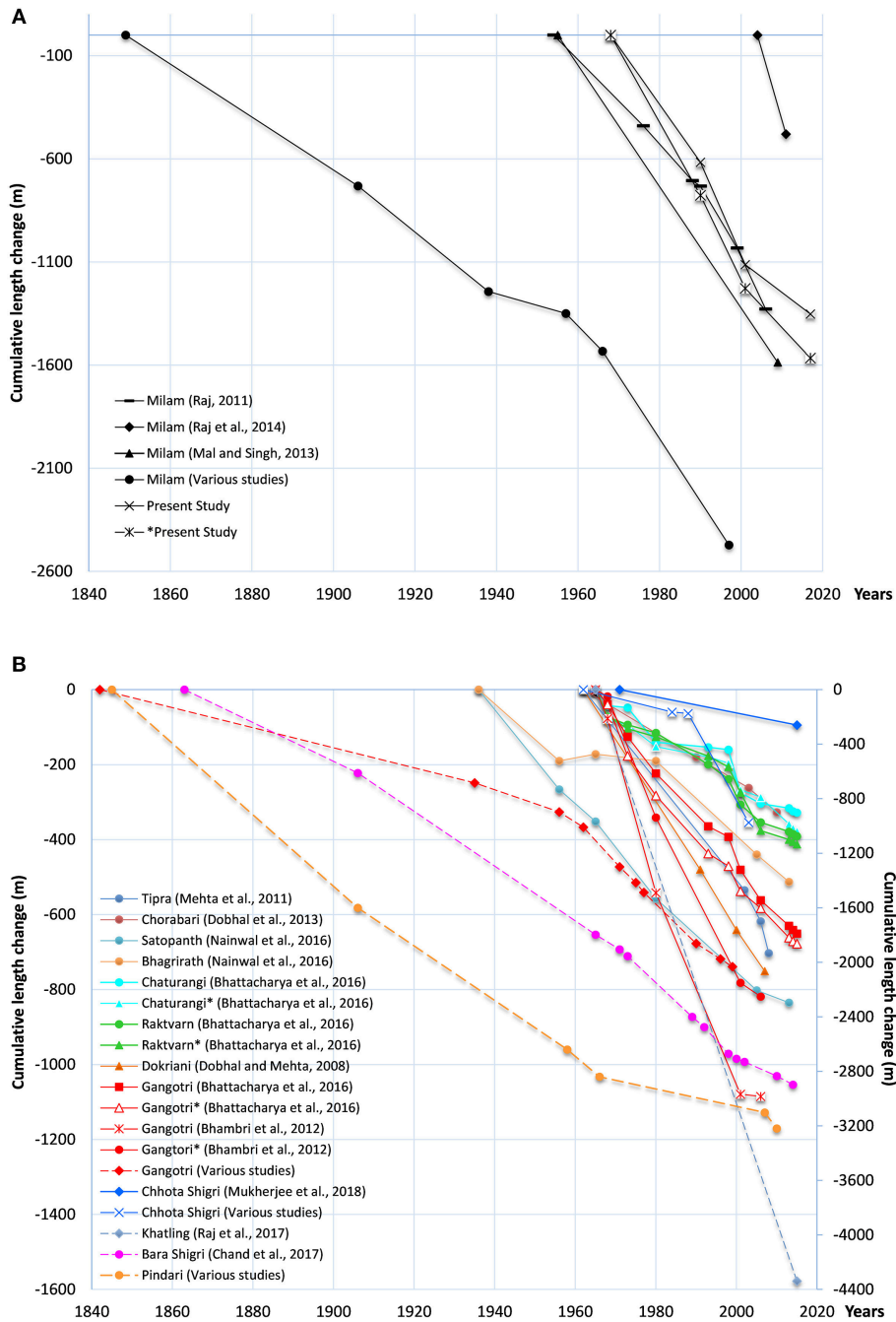


FIGURE 5 | Observed long-term cumulative changes of some of the Himalayan glaciers. **(A)** Shows long-term changes of the Milam glacier based on present and previous studies. **(B)** Indicates long-term changes of nearby glaciers. The markers show the year of observations. The axis on the right side is for the dashed lines. *refers to the studies based on frontal recession. Sources: various studies for the Milam glacier (Cotter and Brown, 1907; Mason, 1939; Jangpangi and Vohra, 1959; Jangpangi, 1975; Shukla and Siddiqui, 2001), the Gangotri glacier (Auden, 1937; Naithani et al., 2001; Srivastava, 2004; Thayyen, 2008; Bhambri and Bolch, 2009), the Pindari glacier (Cotter and Brown, 1907; Tewari and Jangpangi, 1962; Tewari, 1972; Bali et al., 2013), Chhota Shigri (Wadia Institute of Himalayan Geology (WIHG), 1987; Kulkarni et al., 2007; Ramanathan, 2011), based on Bhambri and Bolch (2009) and Chand et al. (2017).

glaciers in Nepal Himalaya increased from 3430 to 5163 between 1980 and 2010 due to the same process. The glaciers detachment has been also observed in the Chenab basin, western Himalaya (Brahmbhatt et al., 2015).

The present study reveals deformation of the moraine ridges caused by glacier thinning. It is observed that the recession of valley glaciers removes the basal support from valley slopes and lateral moraines forming steep trim lines. Thus, valley slopes

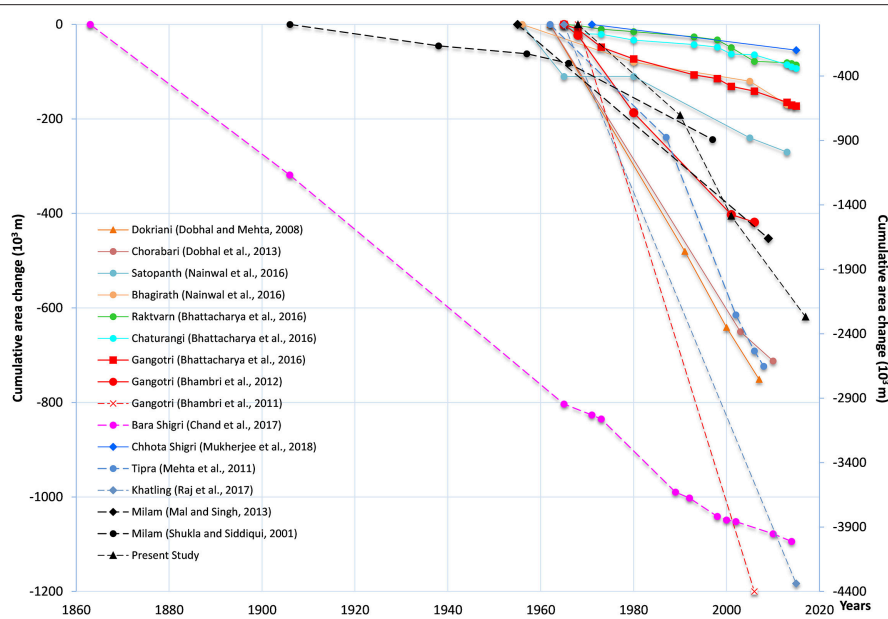


FIGURE 6 | Cumulative area loss of the Milam glacier and some of the Himalayan glaciers. The markers show year of observations. The axis on the right side is for dashed lines.

and moraines overhang the glacier (Ali et al., 2017), which gradually deforms under the force of gravity and their own weight (Evans and Clague, 1994; Pánek and Klimeš, 2016; Lo, 2017). This process may result in failure of large part of moraines (Figure 4A) or slopes, known as deep seated deformation (Pánek and Klimeš, 2016; Lo, 2017) or their shallow degradation (Figure 4B). Slope and moraine deformation increases the thickness and extent of debris cover on the glaciers (Shukla and Qadir, 2016), which over considerable time period modifies the interactions of glacier ice with the atmosphere and its response to changing climate conditions (Scherler et al., 2011; Schmidt and Nüsser, 2012; Dobhal et al., 2013). Similar physical processes of slope deformations have been reported from high latitude glacier regions, e.g., Glacier Bay National Park (Wieczorek et al., 2007), St. Elias Mountain of British Columbia, Alaska region, and Canadian Cordillera (Evans and Clague, 1994), it however remained largely undocumented in the Himalaya (Ali et al., 2017). Our results related to the deformation of moraine ridges caused by glacier thinning, however, need further field investigations.

Climate Change in the Region

The main focus of this study is on the recession of the Milam glacier, however, for a better understanding a brief account of prevailing climate change and its forcings is presented here. The station-based climate data records near the glacier are not available. The long term climate data for the closest stations i.e., Munsyari are either unavailable or show large data gaps (Singh and Mal, 2014), therefore are not usable for understanding climate trends in the region. We therefore used CRU climate data v4.01 (0.5×0.5 -degree, 1968–2016) for the region as recession and fragmentation of the Himalayan glaciers have been

largely attributed to climate change (Bolch et al., 2012, 2019; Kääb et al., 2012, 2015; Bajracharya et al., 2015; Chand et al., 2017). The study shows a mean annual temperature increase of $0.28^\circ\text{C}/\text{decade}$ for the period of 1968 to 2016 (Figure 7), a magnitude considerably higher than global average and nearby regions in the Himalaya. Bhutiyani et al. (2007, 2009) and Bhutiyani (2016) reported an increase of 0.11 to $0.16^\circ\text{C}/\text{decade}$ in mean annual temperature over North-West Himalayan region over the last century. Comparable warming trends of mean annual temperature in West Nepal, close to present study area, (upto $0.6^\circ\text{C}/\text{decade}$) between 1980 and 2009 (Kattel and Yao, 2013) and in the higher elevations of Koshi basin, East Nepal, have been reported between 1975 and 2010 (Shrestha et al., 1999, 2016; Qi et al., 2013). Salerno et al. (2015) revealed an increase of $0.4^\circ\text{C}/\text{decade}$ of mean annual temperature at higher elevations of Everest region, Nepal between 1994 and 2013. The present study shows shallow warming of mean annual temperature in monsoon months compared to other seasons. Comparable warming of monsoon season has been reported in western and central Himalaya in recent decades and over last century (Bhutiyani et al., 2007, 2009; Salerno et al., 2015; Bhutiyani, 2016; Shrestha et al., 2016; Shafiq et al., 2018). Higher warming of post-monsoon followed by pre-monsoon and winter seasons in the region follow the trends akin to western and central Himalaya in recent decades (Salerno et al., 2015; Shrestha et al., 2016; Shafiq et al., 2018).

In the present study, the magnitude of warming is observed to be higher for annual minimum temperatures ($0.46^\circ\text{C}/\text{decade}$) than annual maximum temperature ($0.05^\circ\text{C}/\text{decade}$) over the period 1968–2016. Pronounced warming in minimum temperature is inconsistent with relatively lower elevation based studies of the nearby Himalayan regions (Shrestha et al., 1999; Bhutiyani et al., 2007; Shekhar et al., 2010; Dimri and Dash, 2012;

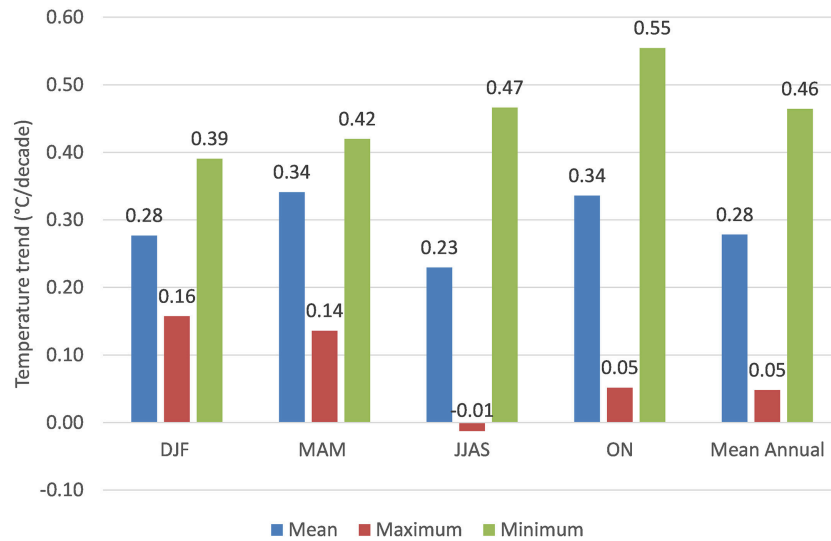


FIGURE 7 | Long-term temperature trends in the study area based on CRU data (1968–2016).

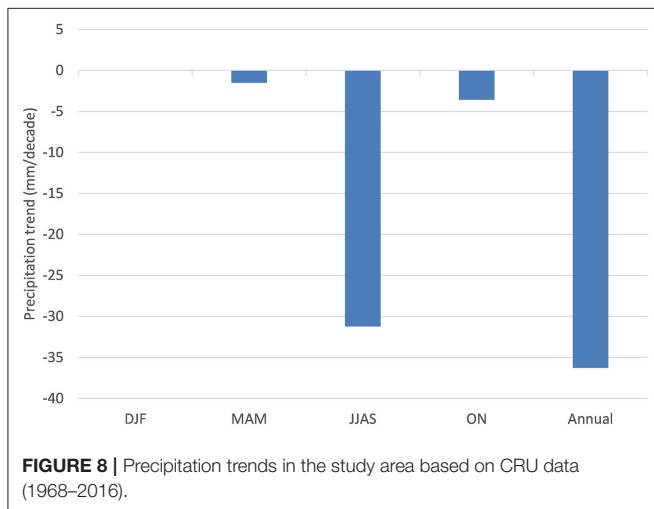


FIGURE 8 | Precipitation trends in the study area based on CRU data (1968–2016).

Kattel and Yao, 2013), but largely corresponds to studies from high elevations (similar elevation ranges to Milam Glacier) in adjacent Himalayan regions (Salerno et al., 2015; Shrestha et al., 2016). In this study, mean minimum temperature rise is recorded highest for post-monsoon season followed by the monsoon, pre-monsoon and winter over the period 1968 and 2016, which are similar to the trends observed for the Everest region by Salerno et al. (2015), while Shafiq et al. (2018) observed the highest warming trends in pre-and post-monsoon seasons followed by winters over western Himalaya between 1973 and 2012. The highest mean maximum temperature trends in this study is recorded in the winters, while the monsoon season is observed to have shallow cooling. On the contrary western Himalaya has recorded highest warming trends in the pre-monsoon season, followed by winters, post-monsoon and monsoon season (Shafiq et al., 2018).

Warming has significant implications on the precipitation form in the higher elevation regions of Himalaya, which greatly influence the snow cover and glaciers (Salerno et al., 2015; Bolch et al., 2019). A study by Bhutiyani (2016) reveals that warming trends in winter has led to declining snowfall contribution to total precipitation, which suggests the possible changes of precipitation form, from snow to rain. The warming of pre- and post-monsoon has particularly reduced snowfall duration by up to 2 weeks and snow cover in the western Himalaya over last three decades (Bhutiyani et al., 2009; Bhutiyani, 2016). Declining snow precipitation amounts reduce snow pack accumulations on the glaciers thereby causing reduced glacier flow and eventually negative mass turnover in long run (Salerno et al., 2015; Bolch et al., 2019). At the same time, the change of precipitation form (snow to rainfall) can accelerate glacier ice melting even at higher elevations, similar to the melting effects on the glacier that of supra and proglacial lakes.

In the present study region, the annual and seasonal precipitation has declined (Figure 8). A significant decline has been observed in the monsoon months, which receive ~62% of total precipitation, followed by post- and pre-monsoon season, while winter precipitation is trendless. The decline in annual and seasonal precipitation in the study area must have caused a reduction in the glacier flow and hence poor ice supply from accumulation zone to the ablation zone, thereby resulting in higher glacier recession. Our results on significant monsoonal precipitation decline are consistent with studies from higher elevations in the Everest region (Salerno et al., 2015), while winter precipitation trends match with the Gangotri region (Bhambri et al., 2011b). We observe distinct seasonal precipitation trends in the region compared with western Himalaya (Bhutiyani et al., 2009) and central Himalaya (Karki et al., 2017). Thus, pronounced warming in the region and changes in precipitation are primarily driving the higher recession rates of the Milam glacier.

CONCLUSION

The recession and associated detachments of glaciers in the Himalaya is of great concern, indicating on the one hand changing climatic conditions at higher elevation, where the meteorological observations are largely unavailable and, affecting on the other hand downstream water availability in long run. Although, number of remote sensing-based studies on Himalayan glaciers have been generally increasing in recent decade, available studies on central Himalayan glaciers are still limited. In this study we analyzed the Milam glacier, which has been subjected to several field and remote sensing data based studies over a century. The study indicates that the Milam glacier has been in a receding phase ($31.9 \pm 0.4 \text{ m a}^{-1}$) over the period 1968–2017, with a relatively lower recession rate ($21.1 \pm 1.7 \text{ m a}^{-1}$) observed in the last two decades. Besides, significant area loss ($2.27 \pm 0.06 \text{ km}^2$), detachment of two tributary glaciers and deformation of moraine ridges in the lower ablation zone, as a result of glacier recession, were observed. We assessed relatively higher long term glacier recession rates compared to those of previous studies on the Milam glacier and on nearby glaciers, which were based on coarse scale topographical maps and coarse-medium resolution satellite data. In addition, observed lower recession rate in recent decades is inconsistent with previous studies on the Milam glacier, although in agreement with nearby glaciers studied using similar data base and methods (based on Bhattacharya et al., 2016). The glacier recession may be influenced by local climatic change processes and topographic factors, leading to significant differences in recession patterns over the period of study. Regional scale study on geodetic mass balance and on the influence of local topography on glacier

recession are required for a more robust understanding of the glacier behavior in the region.

AUTHOR CONTRIBUTIONS

SM and MM conceptualized the study, analyzed the data, wrote and revised the paper. RBS, US, and MPSB conceptualized, reviewed, and revised the paper.

FUNDING

Authors are thankful to DAAD for financial support.

ACKNOWLEDGMENTS

We are thankful to the Institute of Geography, University of Hamburg, for providing the workspace and logistics to conduct this research. MM is also grateful to the Wadia Institute of Himalayan Geology, Dehra Dun, Uttarakhand, for providing the necessary facilities. Further, we acknowledge the valuable comments by reviewers and the discussion with Rakesh Bhambri.

SUPPLEMENTARY MATERIAL

The Supplementary Material for this article can be found online at: <https://www.frontiersin.org/articles/10.3389/fenvs.2019.00042/full#supplementary-material>

Figure S1 | Reduced width of Pacchmi Bamchu glacier at the confluence with the Milam glacier. The width of the confluence was $\sim 253.5 \text{ m}$ in 1968 **(A)**, which decreased to $\sim 110 \text{ m}$ in 2017 **(B)**.

Table S1 | Review of glaciological studies on the Milam glacier.

REFERENCES

- Ageta, Y., and Fujita, K. (1996). Characteristics of mass balance of summer accumulation type glaciers in the Himalaya and Tibet. *Zeitschrift Für Gletscherkunde und Glazialgeologie*. *Band 32*, S61–S65.
- Ageta, Y., and Higuchi, K. (1984). Estimation of mass balance components of a summer-accumulation type glacier in the Nepal Himalaya. *Geogr. Ann. Ser. A Phys. Geogr.* 66, 249–255. doi: 10.1080/04353676.1984.11880113
- Ahmad, N. (1962). “Milam Glacier, Kumaon Himalaya,” in *Variations of the Regime of Existing Glaciers, Symposium of Oberurgl, Commission of Snow and Ice*, Vol. 58, ed W. Ward (Gentbrugge: International Association of Hydrological Science), 230–233.
- Aizen, V. B., Kuzmichenok, V. A., Surazakov, A. B., and Aizen, E. M. (2007). Glacier changes in the Tien Shan as determined from topographic and remotely sensed data. *Glob. Planet. Change* 56, 328–340. doi: 10.1016/j.gloplacha.2006.07.016
- Ali, I., Shukla, A., and Romshoo, S. A. (2017). Assessing linkages between spatial facies changes and dimensional variations of glaciers in the upper Indus Basin, western Himalaya. *Geomorphology* 284, 115–129. doi: 10.1016/j.geomorph.2017.01.005
- Alifu, H., Tateishi, R., and Johnson, B. (2015). A new ban ratio technique for mapping debris-covered glaciers using Landsat imagery and a digital elevation model. *Int. J. Remote Sens.* 36, 2063–2075. doi: 10.1080/2150704X.2015.1034886
- Auden, J. B. (1937). Snout of the Gangotri Glacier, Tehri Garhwal. *Rec. Geol. Survey India* 72, 135–140.
- Azam, M., Wagnon, P., Ramanathan, A. L., Vincent, C., Sharma, P., Arnaud, Y., et al. (2012). From balance to imbalance: a shift in the dynamic behaviour of Chhota Shigri glacier, western Himalaya, India. *J. Glaciol.* 58, 315–324. doi: 10.3189/2012JoG11J123
- Azam, M. F., Wagnon, P., Berthier, E., Vincent, C., Fujita, K., and Kargel, J. S. (2018). Review of the status and mass changes of Himalayan-Karakoram glaciers. *J. Glaciol.* 64, 61–74. doi: 10.1017/jog.2017.86
- Bahuguna, I. M., Kulkarni, A. V., Nayak, S., Rathore, B. P., Negi, H. S., and Mathur, P. (2007). Himalayan glacier retreat using IRS 1C PAN stereo data. *Int. J. Remote Sens.* 28, 437–442. doi: 10.1080/01431160500486674
- Bajracharya, B., Shrestha, A. B., and Rajbhandari, L. (2007). Glacial lake outburst floods in the Sagarmatha region. *Mt. Res. Dev.* 27, 336–344. doi: 10.1659/mrd.0783
- Bajracharya, S. R., Maharjan, S. B., and Shrestha, F. (2014a). The status and decadal change of glaciers in Bhutan from the 1980s to 2010 based on satellite data. *Ann. Glaciol.* 55, 159–166. doi: 10.3189/2014AoG66A125
- Bajracharya, S. R., Maharjan, S. B., Shrestha, F., Bajracharya, O. R., and Baidya, S. (2014b). *Glacier Status in Nepal and Decadal Change From 1980 to 2010 Based on Landsat Data*. Research Report. ICIMOD.
- Bajracharya, S. R., Maharjan, S. B., Shrestha, F., Guo, W., Liu, S., Immerzeel, W., et al. (2015). The glaciers of the Hindu Kush Himalayas: current status and observed changes from the 1980s to 2010. *Int. J. Water Resour. Dev.* doi: 10.1080/07900627.2015.1005731
- Bajracharya, S. R., and Mool, P. (2009). Glaciers, glacial lakes and glacial lake outburst floods in the Mount Everest region, Nepal. *Ann. Glaciol.* 50, 81–86. doi: 10.3189/172756410790595895
- Bali, R., Nawaz, A. S., Agarwal, K. K., Rastogi, S. K., Krishna, K., and Srivastava, P. (2013). Chronology of late Quaternary glaciation in the Pindar valley, Alaknanda basin, Central Himalaya (India). *J. Asian Earth Sci.* 66, 224–233. doi: 10.1016/j.jseas.2013.01.011

- Basistha, A., Arya, D. S., and Goel, N. K. (2009). Analysis of historical changes in rainfall in the Indian Himalayas. *Int. J. Climatol.* 29, 555–572. doi: 10.1002/joc.1706
- Basnett, S., Kulkarni, A., and Bolch, T. (2013). The influence of debris cover and glacial lakes on the recession of glaciers in Sikkim Himalaya, India. *J. Glaciol.* 59, 1035–1046. doi: 10.3189/2013JG12J184
- Bhambri, R., and Bolch, B. (2009). Glacier mapping: a review with special reference to the Indian Himalayas. *Prog. Phys. Geogr.* 33, 672–704. doi: 10.1177/0309133309348112
- Bhambri, R., Bolch, T., and Chaujar, R. K. (2011a). Mapping of debris-covered glaciers in the Garhwal Himalayas using ASTER DEMs and thermal data. *Int. J. Remote Sens.* 32, 8095–8119. doi: 10.1080/01431161.2010.532821
- Bhambri, R., Bolch, T., and Chaujar, R. K. (2012). Frontal recession of Gangotri Glacier, Garhwal Himalayas, from 1965 to 2006, measured through high resolution remote sensing data. *Curr. Sci.* 102, 489–494. doi: 10.5167/uzh-59630
- Bhambri, R., Bolch, T., Chaujar, R. K., and Kulshreshtha, S. C. (2011b). Glacier changes in the Garhwal Himalaya, India, from 1968 to 2006 based on remote sensing. *J. Glaciol.* 57, 543–556. doi: 10.3189/002214311796905604
- Bhambri, R., Bolch, T., Kawishwar, P., Dobhal, D. P., Srivastava, D., and Pratap, B. (2013). Heterogeneity in glacier response in the Shyok valley, northeast Karakoram. *Cryosphere* 7, 1385–1398. doi: 10.5194/tc-7-1385-2013
- Bhambri, R., Hewitt, K., Kawishwar, P., and Pratap, B. (2017). Surge-type and surge-modified glaciers in the Karakoram. *Sci. Rep.* 7:15391. doi: 10.1038/s41598-017-15473-8
- Bhattacharya, A., Bolch, T., Mukherjee, K., Pieczonka, T., Kropáček, J., and Buchroithner, M. F. (2016). Overall recession and mass budget of Gangotri Glacier, Garhwal Himalayas, from 1965 to 2015 using remote sensing data. *J. Glaciol.* 62, 1115–1133. doi: 10.1017/jog.2016.96
- Bhutiyan, M. R. (2016). “Spatial and temporal variability of climate change in high-altitude regions of NW Himalaya,” in *Climate Change, Glacier Response, and Vegetation Dynamics in the Himalaya*, eds R. B. Singh, U. Schickhoff, and S. Mal (Cham: Springer), 87–101.
- Bhutiyan, M. R., Kale, V. S., and Pawar, N. J. (2007). Long-term trends in maximum, minimum and mean annual air temperatures across the Northwestern Himalaya during the twentieth century. *Clim. Change* 85, 159–177. doi: 10.1007/s10584-006-9196-1
- Bhutiyan, M. R., Kale, V. S., and Pawar, N. J. (2009). Climate change and the precipitation variations in the northwestern Himalaya: 1866–2006. *Int. J. Climatol.* 30, 535–548. doi: 10.1002/joc.1920
- Bolch, B., Menounos, B., and Wheate, R. (2010). Landsat-based inventory of glaciers in western Canada, 1985–2005. *Remote Sens. Environ.* 114, 127–137. doi: 10.1016/j.rse.2009.08.015
- Bolch, T., Buchroithner, M., Pieczonka, T., and Kunert, A. (2008). Planimetric and volumetric glacier changes in the Khumbu Himal, Nepal, since 1962 using Corona, Landsat TM and ASTER data. *J. Glaciol.* 54, 592–600. doi: 10.3189/002214308786570782
- Bolch, T., and Kamp, U. (2006). “Glacier mapping in high mountains using DEMs, Landsat and ASTER data,” in *Proceedings of the 8th International Symposium on High Mountain Remote Sensing Cartography*, eds V. Kaufmann and W. Sulzer (Graz: Karl Franzens University), 13–24.
- Bolch, T., Kulkarni, A. V., Käab, A., Huggel, C., Paul, F., Cogley, J. G., et al. (2012). The state and fate of Himalayan Glaciers. *Science* 336, 310–314. doi: 10.1126/science.1215828
- Bolch, T., Pieczonka, T., and Benn, D. I. (2011). Multi-decadal mass loss of glaciers in the Everest area (Nepal Himalaya) derived from stereo imagery. *Cryosphere* 5, 349–358. doi: 10.5194/tc-5-349-2011
- Bolch, T., Shea, J. M., Liu, S., Azam, F. M., Gao, Y., Gruber, S., et al. (2019). “Status and Change of the Cryosphere in the Extended Hindu Kush Himalaya Region,” in *The Hindu Kush Himalaya Assessment*, eds P. Wester, A. Mishra, A. Mukherji, and A. B. Shrestha (Cham: Springer), 209–255.
- Bookhagen, B., and Burbank, D. W. (2010). Toward a complete Himalayan hydrological budget: spatiotemporal distribution of snowmelt and rainfall and their impact on river discharge. *J. Geophys. Res. Earth Sci.* 115, 1–25. doi: 10.1029/2009JF001426
- Brahmbhatt, R. M., Rathore, B. P., Pattniak, S., Jani, P., Bahuguna, I. M., Shah, and R. D., et al. (2015). Peculiar characteristics of fragmentation of glaciers: a case study of Western Himalaya, India. *Int. J. Geosci.* 6, 455–463. doi: 10.4236/ijg.2015.64035
- Brun, F., Berthier, E., Wagnon, P., Käab, A., and Treichler, D. (2017). A spatially resolved estimate of High Mountain Asia glacier mass balances from 2000 to 2016. *Nat. Geosci.* 10, 668–673. doi: 10.1038/ngeo2999
- Buchroithner, M., and Bolch, T. (2007). “An automated method to delineate the ice extension of the debris covered glacier at Mt. Everest based on ASTER imagery,” in *Proceedings of the 9th International Symposium on High Mountain Remote Sensing Cartography* (Graz), 71–78.
- Chand, P., and Sharma, M. C. (2015). Frontal changes in the Manimahesh and Tal Glaciers in the Ravi basin, Himachal Pradesh, northwestern Himalaya (India), between 1971 and 2013. *Int. J. Climatol.* 36, 1049–1113. doi: 10.1080/01431161.2015.1074300
- Chand, P., Sharma, M. C., Bhambri, R., Sangewar, C. V., and Juval, N. (2017). Reconstructing the pattern of the Bara Shigri Glacier fluctuation since the end of the Little Ice Age, Chandra valley, north-western Himalaya. *Prog. Phys. Geogr.* 41, 643–675. doi: 10.1177/0309133317728017
- Cotter, G. D., and Brown, J. C. (1907). “Notes on certain glaciers in Kumaon,” in *Records of Geological Survey of India*, 35 (Calcutta: Government of India), 148–157.
- Dash, S. K., Jenamani, R. K., Kalsi, S. R., and Panda S. K. (2007). Some evidence of climate change in twentieth-century India. *Clim. Change* 85, 299–321. doi: 10.1007/s10584-007-9305-9
- Deota, B. S., Trivedi, Y. N., Kulkarni, A. V., Bahuguna, I. M., and Rathore, B. P. (2011). RS and GIS in mapping of geomorphic records and understanding the local controls of glacial retreat from the Baspa Valley, Himachal Pradesh, India. *Curr. Sci.* 100, 1555–1563.
- Dimri, A. P., and Dash, S. K. (2012). Wintertime climatic trends in the western Himalayas. *Clim. Change* 111, 775–800. doi: 10.1007/s10584-011-0201-y
- Dimri, A. P., Niyogi, D., Barros, A. P., Ridley, J., Mohanty, U. C., Yasunari, T., et al. (2015). Western disturbances: a review. *Rev. Geophys.* 53, 225–246. doi: 10.1002/2014RG000460
- Dimri, A. P., Yasunari, T., Kotlia, B. S., Mohanty, U. C., and Sikka, D. R. (2016). Indian winter monsoon: present and past. *Earth Sci. Rev.* 163, 297–332. doi: 10.1016/j.earscirev.2016.10.008
- Dobhal, D. P., and Mehta, M. (2008). Snout fluctuation of Dokriani Glacier (1962–2007) vis-à-vis the impact of climate change. *Himalayan Geol.* 29, 23–25.
- Dobhal, D. P., Mehta, M., and Srivastava, D. (2013). Influence of debris cover on terminus retreat and mass changes of Chorabari Glacier, Garhwal region, Central Himalaya, India. *J. Glaciol.* 59, 961–971. doi: 10.3189/2013JG12J180
- Dobhal, D. P., Gergan, J. T., and Thayyen, R. J. (2004). Recession and morphogeometrical changes of Dokriani Glacier (1962–1995), Garhwal Himalaya, India. *Curr. Sci.* 86, 692–696.
- Dumka, R. K., Kotlia, B. S., Miral, M. S., Joshi, L. M., Kumar, K., and Sharma, A. K. (2013). First Global Positioning System (GPS) derived recession rate in Milam Glacier, Higher Central Himalaya, India. *Int. J. Eng. Sci.* 2, 58–63.
- Dutta, S., Ramanathan, A. L., and Linda, A. (2012). Glacier fluctuation using Satellite Data in Beas basin, 1972–2006, Himachal Pradesh, India. *J. Earth Syst. Sci.* 121, 1105–1112. doi: 10.1007/s12040-012-0219-1
- Evans, S. G., and Clague, J. (1994). Recent climatic change and catastrophic geomorphic processes in mountain environments. *Geomorphology* 10, 107–128. doi: 10.1016/0169-555X(94)90011-6
- Frey, H., Paul, F., and Strozzi, T. (2012). Compilation of a glacier inventory for the western Himalayas from satellite data: methods, challenges, and results. *Remote Sens. Environ.* 124, 832–843. doi: 10.1016/j.rse.2012.06.020
- Fujita, K., Sakai, A., Nuimura, T., Yamaguchi, S., and Sharma, R. R. (2009). Recent changes in Imja Glacial Lake and its damming moraine in the Nepal Himalaya revealed by *in situ* surveys and multi-temporal ASTER imagery. *Environ. Res. Lett.* 4:045205. doi: 10.1088/1748-9326/4/4/045205
- Gardelle, J., Berthier, E., and Arnaud, Y. (2012). Slight mass gain of Karakoram glaciers in the early twenty-first century. *Nat. Geosci.* 5, 322–325. doi: 10.1038/ngeo1450
- Granshaw, F. D., and Fountain, A. G. (2006). Glacier change (1958–1998) in the North Cascades National Park Complex, Washington, USA. *J. Glaciol.* 52, 251–256. doi: 10.3189/172756506781828782
- Guo, X., Wang, L., and Tian, L. (2016). Spatio-temporal variability of vertical gradients of major meteorological observations around the Tibetan Plateau. *Int. J. Climatol.* 36, 1901–1916. doi: 10.1002/joc.4468

- Hall, D. K., Bahr, K. J., Shoener, W., Bindschadler, R. A., and Chien, J. Y. L. (2003). Consideration of the errors inherent in mapping historical glacier positions in Austria from the ground and space. *Remote Sens. Environ.* 86, 566–577. doi: 10.1016/S0034-4257(03)00134-2
- Hall, D. K., Riggs, G. A., and Salomonson, V. V. (1995). Development of methods for mapping global snow cover using moderate resolution imaging spectroradiometer data. *Remote Sens. Environ.* 54, 127–140. doi: 10.1016/0034-4257(95)00137-P
- Heim, A., and Gansser, A. (1939). *The Throne of the Gods: An Account of the First Swiss Expedition to the Himalayas*. New York, NY: The Macmillan Company.
- Hewitt, K. (2007). Tributary glacier surges: an exceptional concentration at Panmah Glacier, Karakoram Himalaya. *J. Glaciol.* 53, 181–188. doi: 10.3189/172756507782202829
- IPCC (2013). *Climate Change 2013: The Physical Science Basis*. Contribution of Working Group I to the Fifth Assessment Report of the Intergovernmental Panel on Climate Change, eds T. F. Stocker, T. F. D. Qin, G.-K. Plattner, M. Tignor, S. K. Allen, J. Boschung, A. Nauels, Y. Xia, V. Bex, and P. M. Midgley. Cambridge: New York, NY, Cambridge University Press.
- Jangpangi, B. S. (1958). Report on the survey and glaciological study of the Gangotri glacier, Tehri Garhwal District: Glacier No. 3, Arwa Valley: Satopanth and Bhagirath Kharak Glaciers, Garhwal District, Uttar Pradesh. *Mem. Geol. Survey India* 18.
- Jangpangi, B. S. (1975). A Note on the observations made on some glaciers of Malla Johar in 1966. *Rec. Geol. Survey India* 106, 240–247.
- Jangpangi, B. S., and Vohra, C. P. (1959). *Report on Glaciological Study of Milam, Poting and Shankalpa (Ralam) Glaciers, Pithoragarh District, Uttar Pradesh*. Lucknow: Geological Survey of India.
- Jin, R., Li, X., Che, T., Wu, L., and Mool, P. (2005). Glacier area changes in the Pumqu river basin, Tibetan Plateau, between the 1970s and 2001. *J. Glaciol.* 5, 607–610. doi: 10.3189/172756505781829061
- Kääb, A., Berthier, E., Nuth, C., Gardelle, J., and Arnaud, Y. (2012). Contrasting patterns of early twenty first-century glacier mass change in the Himalayas. *Nature* 488, 495–498. doi: 10.1038/nature11324
- Kääb, A., Treichler, D., Nuth, C., and Berthier, E. (2015). Brief communication: contending estimates of 2003–2008 glacier mass balance over the Pamir-Karakoram-Himalaya. *Cryosphere* 9, 557–564. doi: 10.5194/tc-9-557-2015
- Kamp, U., Byrjn, M., and Bolch, T. (2011). Glacier Fluctuations between 1975 and 2008 in the Greater Himalaya Range of Zaskar, Southern Ladakh. *J. Mt. Sci.* 8, 374–389. doi: 10.1007/s11629-011-2007-9
- Karki, R., Hasson, S., Schickhoff, U., Scholten, T., and Jürgen, B. (2017). Rising precipitation extremes across Nepal. *Climate* 5:4. doi: 10.3390/cli5010004
- Kattel, D. B., and Yao, Y. (2013). Recent temperature trends at mountain stations on the southern slope of the central Himalayas. *J. Earth Syst. Sci.* 122, 215–227. doi: 10.1007/s12040-012-0257-8
- King, O., Dehecq, A., Quincey, D., and Carrivick, J. (2018). Contrasting geometric and dynamic evolution of lake and land-terminating glaciers in the central Himalaya. *Glob. Planet. Change.* 167, 46–60. doi: 10.1016/j.gloplacha.2018.05.006
- King, O., Quincey, D. J., Carrivick, J. L., and Rowan, A. V. (2017). Spatial variability in mass loss of glaciers in the Everest region, central Himalayas, between 2000 and 2015. *Cryosphere* 11, 407–426. doi: 10.5194/tc-11-407-2017
- Kothawale, D. R., and Rupa Kumar, K. (2005). On the recent changes in surface temperature trends over India. *Geophys. Res. Lett.* 32:L18714. doi: 10.1029/2005GL023528
- Kulkarni, A. V., and Bahuguna, I. M. (2002). Glacial retreat in the Baspa basin, Himalaya, monitored with satellite stereo data. *J. Glaciol.* 48, 171–172. doi: 10.3189/172756502781831601
- Kulkarni, A. V., Bahuguna, I. M., Rathore, B. P., Singh, S. K., Randhawa, S. S., Sood, R. K., et al. (2007). Glacial retreat in Himalayas using Indian remote sensing satellite data. *Curr. Sci.* 92, 69–74.
- Kulkarni, A. V., and Karyakarte, Y. (2014). Observed changes in Himalayan glaciers. *Curr. Sci.* 106, 237–244.
- Kumar, G., Mehdi, S. H., and Prakash, G. (1975). Observations of the some glaciers of Kumaon Himalaya, U.P. *Rec. Geol. Survey India* 106, 231–239.
- Lo, C. M. (2017). Evolution of deep-seated landslide at Putanpunas stream, Taiwan. *Geomat. Nat Hazards Risk* 8, 1204–1224. doi: 10.1080/19475705.2017.1309462
- Mal, S., and Singh, R. B. (2013). “Differential recession of glaciers in Nanda Devi biosphere reserve, Garhwal Himalaya, India; in *Cold and Mountain Region Hydrological Systems under Climate Change: Towards Improved Projections*. IAHS Publication 360. *Proceedings of H02, IAHS-IAPSO-IASPEI Assembly* (Gothenburg), 71–76.
- Mason, K. (1939). Progress of Himalayan surveys. *Himalayan J.* 11, 169–171.
- Mayewski, P. A., and Jeschke, P. A. (1979). Himalayan and Trans-Himalayan glacier fluctuations since AD 1812. *Arctic Alpine Res.* 11, 267–287. doi: 10.2307/1550417
- Mehta, M., Dobhal, D. P., and Bisht, M. P. S. (2011). Change of Tipra Glacier in the Garhwal Himalaya, India, between 1962 and 2008. *Prog. Phys. Geogr.* 35, 721–738. doi: 10.1177/0309133311411760
- Mehta, M., Dobhal, D. P., Kesarwani, K., Pratap, B., Kumar, A., and Verma, A. (2014). Monitoring of glacier changes and response time in Chorabari Glacier, Central Himalaya, Garhwal, India. *Curr. Sci.* 107, 281–289. doi: 10.13140/2.1.4435.0083
- Mehta, M., Dobhal, D. P., Pratap, B., Verma, A., Kumar, A., and Srivastava, D. (2012a). Glacier changes in upper Tons river basin, Garhwal Himalaya, Uttarakhand, India. *Zeitschr. Geomorphol.* 57, 225–244. doi: 10.1127/0372-8854/2012/0095
- Mehta, M., Majeed, Z., Dobhal, D. P., and Srivastava, P. (2012b). Geomorphological evidences of post LGM glacial advancement in the Himalaya: a study from Chorabari glacier, Garhwal Himalaya. *Indian J. Earth Syst. Sci.* 121, 149–163. doi: 10.1007/s12040-012-0155-0
- Mir, R. A., and Majeed, Z. (2016). Frontal recession of Parkachik glacier between 1971–2015, Zaskar Himalaya using remote sensing and field data. *Geocarto Int.* 33, 1–15. doi: 10.1080/10106049.2016.1232439
- Mukherjee, K., Bhattacharya, A., Pieczonka, T., Ghosh, S., and Bolch, T. (2018). Glacier mass budget and climate reanalysis data indicate a climatic shift around 2000 in Lahaul-Spiti, western Himalaya. *Clim. Change* 148, 219–233. doi: 10.1007/s10584-018-2185-3
- Mukul, M., Srivastava, V., Jade, S., and Kukul, M. (2017). Uncertainties in the Shuttle Radar Topography Mission (SRTM) Heights: insights from the Indian Himalaya and Peninsula. *Sci. Rep.* 7:41672. doi: 10.1038/srep41672
- Nainwal, H. C., Banerjee, A., Shankar, R., Semwal, P., and Sharma, T. (2016). Shrinkage of Satopanth and Bhagirath Kharak glaciers, India, from 1936 to 2013. *Ann. Glaciol.* 57, 131–139. doi: 10.3189/2016AoG71A015
- Naithani, A. K., Nainwal, H. C., Sati, K. K., and Prasad, C. (2001). Geomorphological evidences of retreat of the Gangotri glacier and its characteristics. *Curr. Sci.* 80, 87–94.
- Nie, Y., Sheng, Y., Liu, Q., Liu, L., Liu, S., Zhang, Y., et al. (2017). A regional-scale assessment of Himalayan glacial lake changes using satellite observations from 1990 to 2015. *Remote Sens. Environ.*, 189, 1–13. doi: 10.1016/j.rse.2016.11.008
- Owen, L., Derbyshire, E., Richardson, S., Benn, D. I., Evans, D. J. A., and Mitchell, W. A. (1996). The Quaternary glacial history of the Lahul Himalaya, northern India. *J. Quat. Sci.* 11, 25–42.
- Palazzi, E., Hardenberg, J. V., and Provenzale, A. (2013). Precipitation in the Hindu-Kush Karakoram Himalaya: observations and future scenarios. *J. Geophys. Res. Atmos.* 118, 85–100. doi: 10.1029/2012JD018697
- Pandey, A. C., Ghosh, S., and Nathawat, M. S. (2011). Evaluating patterns of temporal glacier changes in Greater Himalayan Range, Jammu and Kashmir, India. *Geocarto Int.* 26, 321–338. doi: 10.1080/10106049.2011.554611
- Pandey, P., and Venkataraman, G. (2013). Changes in the glaciers of Chandra-Bhaga basin, Himachal Himalaya, India, between 1980 and 2010 measured using remote sensing. *Int. J. Remote Sens.* 34, 5584–5597. doi: 10.1080/01431161.2013.793464
- Pánek, T., and Klimeš, J. (2016). Temporal behavior of deep-seated gravitational slope deformations: a review. *Earth Sci. Rev.* 156, 14–38. doi: 10.1016/j.earscirev.2016.02.007
- Paul, F., Barrand, N. E., Baumann, S., Berthier, E., Bolch, T., Casey, K., et al. (2013). On the accuracy of glacier outlines derived from remote-sensing data. *Ann. Glaciol.* 54, 171–182. doi: 10.3189/2013AoG63A296
- Paul, F., Bolch, T., Briggs, K., Kääb, A., McMillan, M., McNabb, R., et al. (2017). Error sources and guidelines for quality assessment of glacier area, elevation change, and velocity products derived from satellite data in the Glaciers_cci

- project. *Remote Sens. Environ.* 203, 256–275. doi: 10.1016/j.rse.2017.08.038
- Paul, F., Huggel, C., and Kääb, A. (2004). Combining satellite multispectral image data and a digital elevation model for mapping Debris-covered Glaciers. *Remote Sens. Environ.* 89, 510–518. doi: 10.1016/j.rse.2003.11.007
- Pieczonka, T., and Bolch, T. (2015). Region-wide glacier mass budgets and area changes for the Central Tien Shan between ~ 1975 and 1999 using Hexagon KH-9 imagery. *Glob. Planet. Change* 128, 1–13. doi: 10.1016/j.gloplacha.2014.11.014
- Qi, W., Zhang, Y., Gao, J., Yang, X., Liu, L., and Khanal, N. R. (2013). Climate change on the southern slope of Mt. Qomolangma (Everest) Region in Nepal since 1971. *J. Geogr. Sci.* 23, 595–611. doi: 10.1007/s11442-013-1031-9
- Quincey, D. J., Glasser, N. F., Cook, S. J., and Luckman, A. (2015). Heterogeneity in Karakoram glacier surges. *J. Geophys. Res. Earth Surf.* 120, 1288–1300. doi: 10.1002/2015JF003515
- Raina, V. K. (2010). *MoEF Discussion Paper: Himalayan Glaciers-A State-of-Art Review of Glacial Studies, Glacial Retreat and Climate Change*. Ministry of Environment and Forests and GB Pant Institute of Himalayan Environment and Development, Almora.
- Raj, K. B. G. (2011). Recession and reconstruction of Milam glacier, Kumaon Himalaya, observed with satellite imagery. *Curr. Sci.* 100, 1420–1425.
- Raj, K. B. G., Kumar, K. V., Mishra, R., and Mukhtar, M. A. (2014). Remote sensing based assessment of glacial lake growth on Milam Glacier, Goriganga Basin, Kumaon Himalaya. *J. Geol. Soc. India* 83, 385–392. doi: 10.1007/s12594-014-0055-9
- Raj, K. B. G., Rao, V. V. N., Kumar, K. V., and Diwakar, P. G. (2017). Alarming recession of glaciers in Bhilangna basin, Garhwal Himalaya, from 1965 to 2014 analysed from Corona and Cartosat data. *Geomat. Nat. Hazards Risk* 8, 1424–1439. doi: 10.1080/19475705.2017.1339736
- Ramanathan, A. L. (2011). *Status Report on Chhota Shigri Glacier (Himachal Pradesh)*, Department of Science and Technology. Ministry of Science and Technology, New Delhi. Himalayan Glaciology Technical Report 1, 1–88.
- Rastner, P., Bolch, T., Totarnicola, C., and Paul, F. (2014). A comparison of pixel- and object-based glacier classification with optical satellite images. *IEEE J. Select. Top. Appl. Earth Observ. Remote Sens.* 7, 853–862. doi: 10.1109/JSTARS.2013.2274668
- Robson, B. A., Nuth, C., Dahl, S. O., Hölbling, D., Strozzi, T., and Nielsen, P. R. (2015). Automated classification of debris-covered glaciers combining optical, SAR and topographic data in an object-based environment. *Remote Sens. Environ.* 170, 372–387. doi: 10.1016/j.rse.2015.10.001
- Rodriguez, E., Morris, C. S., and Belz, J. E. (2006). A global assessment of the SRTM performance. *Photogramm. Eng. Remote Sens.* 72, 249–260. doi: 10.14358/PERS.72.3.249
- Sakai, A., Nishimura, K., Kadota, T., and Takeuchi, N. (2009). Onset of calving at supraglacial lakes on debris-covered glaciers of the Nepal Himalaya. *J. Glaciol.* 55, 909–917. doi: 10.3189/002214309790152555
- Salerno, F., Guyennon, N., Thakuri, S., Viviano, G., Romano, E., Vuillermoz, E., et al. (2015). Weak precipitation, warm winters and springs impact glaciers of south slopes of Mt. Everest (central Himalaya) in the last 2 decades (1994–2013). *Cryosphere* 9, 1229–1247. doi: 10.5194/tc-9-1229-2015
- Scherler, D., Bookhagen, B., and Strecker, M. R. (2011). Spatially variable response of Himalayan glaciers to climate change affected by debris cover. *Nat. Geosci. Lett.* 4, 156–159. doi: 10.1038/NCEO1068
- Schickhoff, U., Singh, R. B., and Mal, S. (2016). “Climate change and dynamics of glaciers and vegetation in the Himalaya: an overview,” in *Climate Change, Glacier Response, and Vegetation Dynamics in the Himalaya*, eds R. B. Singh, U. Schickhoff, and S. Mal, (Cham: Springer) 1–26.
- Schmidt, S., and Nüsser, M. (2012). Fluctuations of Raikot Glacier during the past 70 years: a case study from the Nanga Parbat massif, northern Pakistan. *J. Glaciol.* 55, 949–959. doi: 10.3189/002214309790794878
- Scott, C. A., Zhang, F., Mukherji, A., Immerzeel, W., Mustafa, D., and Bharati, L. (2019). “Water in the Hindu Kush Himalaya,” in *The Hindu Kush Himalaya Assessment: Mountains, Climate Change, Sustainability and People*, eds P. Wester, A. Mishra, A. Mukherji, and A. B. Shrestha (Cham: Springer International Publishing), 257–299.
- Shafiq, M. U., Rasool, R., Ahmed, P., and Dimri, A. P. (2018). Temperature and Precipitation trends in Kashmir valley, North Western Himalayas. *Theor. Appl. Climatol.* 135, 293–304. doi: 10.1007/s00704-018-2377-9
- Shekhar, M., Chand, H., Kumar, S., Srinivasan, K., and Ganju, A. (2010). Climate-change studies in the western Himalaya. *Ann. Glaciol.* 51, 105–112. doi: 10.3189/172756410791386508
- Shipton, E. (1935). Nanda Devi and the Ganges Watershed. *Geogr. J.* 85, 305–319. doi: 10.2307/1785589
- Shrestha, A. B., Bajracharya, S. R., Sharma, A. R., Duo, C., and Kulkarni, A. (2016). Observed trends and changes in daily temperature and precipitation extremes over the Koshi river basin 1975–2010. *Int. J. Climatol.* 37, 1066–1083. doi: 10.1002/joc.4761
- Shrestha, A. B., Wake, C. P., Mayewski, P. A., and Dibb, A. E. (1999). Maximum temperature trends in the Himalaya and its vicinity: an analysis based on temperature records from Nepal for the Period 1971–94. *J. Clim.* 12, 2275–2286.
- Shukla, A., Arora, M. K., and Gupta, R. P. (2010). Synergistic approach for mapping debris-covered glaciers using optical-thermal remote sensing data with inputs from geomorphometric parameters. *Remote Sens. Environ.* 114, 1378–1387. doi: 10.1016/j.rse.2010.01.015
- Shukla, A., and Qadir, J. (2016). Differential response of glaciers with varying debris cover extent: evidence from changing glacier parameters. *Int. J. Remote Sens.* 37, 2453–2479. doi: 10.1080/01431161.2016.1176272
- Shukla, S. P., and Siddiqui, M. A. (2001). “Recession of the Snout Front of Milam Glacier, Goriganga Valley, District Pithoragarh, Uttar Pradesh,” in *Proceedings of Symposium on Snow, Ice and Glaciers- A Himalayan Perspective* (Lucknow: Geological Survey of India), 71–75.
- Singh, R. B., and Mal, S. (2014). Trends and variability of monsoon and other rainfall seasons in Western Himalaya, India. *Atmos. Sci. Lett.* 15, 218–226. doi: 10.1002/asl2.494
- Srivastava, D. (2004). “Recession of Gangotri glacier,” in *Proceedings of Workshop on Gangotri Glacier, Lucknow 26-28 March, 2003. Geological Survey of India Special Publication 80*, eds D. Srivastava, K. R. Gupta, and S. Mukerji (Lucknow: Geological Survey of India), 21–32.
- Tewari, A. P. (1972). Recent changes in the positions of snout of the pindari glacier, Kumaon Himalaya, Almora district, Uttar Pradesh, India. in *Proceedings of the Banff Symposia, Role of Snow and Ice in Hydrology* (Banff, AB: UNESCO-WMO-IAHS, IAHS publication), 1144–1149.
- Tewari, A. P., and Jangpangi, B. S. (1962). “The retreat of the snout on the Pindari Glacier,” in *Variations of the Regime of Existing Glaciers, Symposium of Obergurgl, Commission of Snow and Ice*, Vol. 58. ed W. Ward (Gentbrugge: International Association of Hydrological Sciences), 245–248.
- Thakuri, S., Salerno, F., Smiraglia, C., Bolch, T., D’Agata, C., Viviano, G., et al. (2014). *Tracing glacier changes since the 1960s on the south slope of Mt. Everest (central Southern Himalaya) using optical satellite imagery. Cryosphere* 8, 1297–1315.
- Thayyen, R. J. (2008). Lower recession rate of Gangotri glacier during 1971–2004. *Curr. Sci.* 95, 9–10.
- Thayyen, R. J., and Gergan, J. T. (2010). Role of glaciers in watershed hydrology: a preliminary study of a Himalayan catchment. *Cryosphere* 4, 115–128. doi: 10.5194/tc-4-115-2010
- US Army (1954). *Topographic Map, NH 44-6 (1:250000), Series U502, Based on Medium Scale Ground Controlled Survey During 1924–1943*. Washington, DC: US Army Corps of Engineers,
- Venkatesh, T. N., Kulkarni, A. V., and Srinivasan, J. (2013). Relative effect of slope and equilibrium line altitude on the retreat of Himalayan glaciers. *Cryosphere* 6, 301–311. doi: 10.5194/tc-6-301-2012
- Vohra, C. P. (1980). “Some problems of glacier inventory in the Himalayas,” in *Proceedings of the Riederl Workshop*, Vol. 126 (Washington, DC: IAHS-AISH Publication), 67–74.
- Wadia Institute of Himalayan Geology (WIHG) (1987). *Generation Cum Interpretation of Geophysical Potential Field (Bouguer Anomalies) by Theoretical Methods in Chhota Shigri*. Technical report on Multi-Disciplinary glacier expedition to Chhota Shigri, Department of Science and Technology. 199–215.

- Wang, L., Li, Z., Wang, F., and Edwards, R. (2014). Glacier shrinkage in the Ebinur lake basin, Tien Shan, China, during the past 40 years. *J. Glaciol.* 60, 245–254. doi: 10.3189/2014JoG13J023
- Wieczorek, G. F., Geist, E. L., Motyka, R. J., and Matthias, J. (2007). Hazard assessment of the Tidal Inlet landslide and potential subsequent tsunami, Glacier Bay National Park, Alaska. *Landslides* 4, 205–215. doi: 10.1007/s10346-007-0084-1
- Ye, Q., Kang, S., Chen, F., and Wang, J. (2006). Monitoring glacier variations on Geladandong mountain, central Tibetan Plateau, from 1969 to 2002 using remote-sensing and GIS technologies. *J. Glaciol.* 52, 537–545. doi: 10.3189/172756506781828359

Conflict of Interest Statement: The authors declare that the research was conducted in the absence of any commercial or financial relationships that could be construed as a potential conflict of interest.

Copyright © 2019 Mal, Mehta, Singh, Schickhoff and Bisht. This is an open-access article distributed under the terms of the Creative Commons Attribution License (CC BY). The use, distribution or reproduction in other forums is permitted, provided the original author(s) and the copyright owner(s) are credited and that the original publication in this journal is cited, in accordance with accepted academic practice. No use, distribution or reproduction is permitted which does not comply with these terms.